IEEE Access
Multidisciplinary | Rapid Review | Open Access Journal

Received January 16, 2021, accepted January 29, 2021, date of publication February 9, 2021, date of current version February 18, 2021.

Digital Object Identifier 10.1109/ACCESS.2021.3058151

A Review of Metasurfaces for Microwave Energy Transmission and Harvesting in Wireless Powered Networks

AKAA AGBAEZE ETENG[1], (Member, IEEE), HUI HWANG GOH[2], (Senior Member, IEEE), SHARUL KAMAL ABDUL RAHIM[3], (Senior Member, IEEE), AND AKRAM ALOMAINY[4], (Senior Member, IEEE)

[1]Department of Electrical/Electronic Engineering, Faculty of Engineering, University of Port Harcourt, Choba 500102, Nigeria
[2]School of Electrical Engineering, Guangxi University, Nanning 530004, China
[3]Wireless Communication Centre, Faculty of Electrical Engineering, Universiti Teknologi Malaysia, Johor Bahru 81310, Malaysia
[4]Antennas and Electromagnetics Research Group, School of Electronic Engineering and Computer Science, Queen Mary University of London, London E1 4NS, U.K.

Corresponding author: Hui Hwang Goh (hhgoh@gxu.edu.cn)

This work was supported in part by the School of Electrical Engineering, Guangxi University under Grant A3020051008, and in part by the Kementerian Pengajian Tinggi (KPT) and Universiti Teknologi Malaysia under Grant 5F237 and Grant 3F508.

ABSTRACT Wireless energy transmission and harvesting techniques have recently emerged as attractive solutions to realize wireless powered networks. By eliminating fundamental power constraints arising from the use of conventionally battery sources, wireless modes of energy transmission provide viable means to power wireless network devices away from the grid. Metasurfaces have emerged as key enablers for the use of microwave energy as a power source. Their unique abilities to tailor electromagnetic waves have motivated significant research interest into their use for power-focused microwave systems. This article provides an overview of progress in the development of metasurface implementations for microwave energy transmitters and energy harvesters. First, the paper provides a basic introduction to metasurfaces, after which it reviews research progress in metasurfaces for microwave energy transmission and harvesting. Also highlighted are key parameters by which the performance of such metasurface designs are characterized. In addition, an overview of studies on metasurfaces as reconfigurable intelligent surfaces in wireless networks supporting the simultaneous transmission of information and energy is presented. Finally, the paper highlights existing challenges, and explores future directions, including opportunities to control radio environments through ambiently energized reconfigurable intelligent surfaces in next-generation wireless networks.

INDEX TERMS Energy harvesting, metasurface, microwave power transfer, rectenna, wireless powered networks.

I. INTRODUCTION

Next-generation wireless networks are envisaged as a convergence of communication, environmental sensing and distributed computation [1], with the ability to support a wide range of novel applications [2], [3]. Expectedly, these future networks will be characterized by a considerable heterogeneity of participating nodes [4], [5], each with varied power requirements. For over half a century, batteries have been the de-facto means by which standalone devices were energized without being connected to the grid. However, over the past decade, novel wireless network applications have arisen, which necessitate the placement of various devices in physically inaccessible environments. Such scenarios often negate the possibility of human intervention to facilitate the replacement of limited life-span batteries [6], [7]. Some other applications have stringent restrictions [8], for which additional battery payloads are impractical. It has, therefore, become necessary to investigate wireless and battery-less alternatives for energizing standalone devices [9].

There are numerous energy sources available in the environment. Solar irradiation, wind and tidal waves are some well-known examples, with mature technologies available for harnessing them on a large scale. However, the near-pervasive

The associate editor coordinating the review of this manuscript and approving it for publication was Marco Martalo.

availability of wireless communication technologies globally has provided a largely untapped energy resource to the environment – artificially generated electromagnetic (EM) waves [10]. The EM energy arising from wireless communication technologies is available over a wide spectrum, ranging from radio waves in the kHz regime, to optical wavelengths at THz frequencies. The microwave spectral window, in particular, hosts a significant number of wireless services. Although the ambient energy levels of radiations in this regime are typically kept low by regulation, networked low-power devices can benefit from harnessing ambient EM waves, and intentional EM transmission as a wireless energy source [11]–[14].

Sourcing electrical power from EM transmissions is an idea often traced to the pioneering work of Tesla at the dawn of the 20th century [15]. Although hampered by the available technology of the day [16], these early attempts provided the impetus for further attempts to actualize the idea. Although initial efforts were geared towards realizing technologies for wireless power transfer (WPT) through intentional EM energy transmission, the research has since broadened to include scavenging ambient EM energy made available by a plethora of wireless communication technologies, otherwise known as EM energy harvesting. Microwave power transfer (MPT) is traditionally viewed as a subset of WPT technologies, focusing on transmitter and receiver designs for power transfer at microwave frequencies over relatively considerable distances. Practical MPT realizations, pioneered by W. C. Brown, were initially geared towards high-power applications, including the remote powering of unmanned aerial vehicles (UAVs), and various space solar power (SSP) applications [15], [17]–[19]. However, the basic concept has broadened in contemporary times, to include mid-power and low-power applications, especially in the context of wireless powered communications networks [20]–[24].

Highly focused energy beams from specially synthesized EM apertures could enable the energizing of intended devices placed within the immediate vicinity of these sources. Dedicated long-distance microwave energy transmission links, however, face the challenge of high propagation loss. This is due to that fact that, in the far-field, transmitted power decays with the square of distance. Mitigating this challenge by transmitting high-power directional beams in terrestrial, and residential environments raises obvious safety concerns. Alternatively, existing microwave sources within the wireless network can be harnessed for energizing connected devices. However, given that these technologies are necessarily subject to exposure limits by regulation, the potential for reliable point-to-multipoint microwave energy transmission pales the farther intended devices are from these sources. Far-field MPT in wireless powered networks must satisfactorily address high propagation losses and safety considerations in order to be deployed as viable solutions [20]. Consequently, in far-field scenarios, it is more practical for intended devices to harvest ambient microwave energy made available by multiple sources, rather than depend on a dedicated energy delivery transmission.

Microwave energy harvesting is preoccupied with gathering low-power ambient emissions, with an implementation focus on the development of appropriate energy receivers. Conventionally, the EM energy collectors are antennas. A rectifier is typically included in the antenna structure, thereby yielding a rectenna whose output is a DC voltage.

Antenna structures designed for microwave energy transmission are generally characterized by various implementation complexities. As energy harvesters, it is often the case that antennas are used in arrays to increase the amount of collected power. Such array implementations often require significant spacing between adjacent antenna elements to avoid the debilitating impact of mutual coupling. This places constraints on the number of antenna elements to be used within a finite footprint, or alternatively, on the minimum footprint occupied by an array of a specified number of elements. Also, array rectenna implementations usually require additional matching circuits and power combining networks, leading to complicated designs, higher power losses, and higher costs. Consequently, the need to more efficiently transmit and recover microwave energy, given the regulated wireless ecosystem, has led to investigations into the use of metamaterial-based structures to either supplement antenna functionality, or as outright antenna replacements.

One of the attractive features of planar metamaterials is their ability to realize spatial processing of energy beams without the need for amplifiers or active phase shifters [25], thereby enabling energy efficient power transfer at minimal costs. Also, these structures can be synthesized with less stringent spacing requirements for the constituent elements than antenna arrays, leading to denser configurations and smaller overall footprints. Furthermore, they present greater structural flexibility, which can be exploited to match impedances without using extra circuitry.

As implied in the name, metamaterials are 3D structures with artificially engineered EM properties not found in nature [26]. Their numerous applications in microwave and optical domains are well documented [27]–[29]. Metasurfaces are the 2D equivalents of metamaterials, and have often served as their structurally more compact replacements. Some examples of metasurface applications include the realization of impedance-matching surfaces, electromagnetic absorbers, waveguides, lenses, cloaking materials, antennas, modulators and reconfigurable intelligent surfaces, as summarized in [30]–[32].

WPT and EM energy harvesting applications of metasurfaces and metamaterials have attracted numerous contributions, as outlined in recent surveys [33]–[35]. Li *et al.* [33] reviews research progress in the use of metasurfaces for ambient electromagnetic energy harvesting and WPT, with emphasis placed on energy harvesting applications. Structural simplicity and excellent performance are noted as some reasons for the growing interest in the application of metasurfaces for EM energy harvesting. Similarly, Amer *et al.* [34], provides a summary of metasurface-based radio-frequency energy harvesting designs, which is preceeded by an outlining

of the shortcomings of conventional energy harvesting rectennas. By contrast, the authors in [35] review the fundamentals, progress, and future directions in metamaterial-assisted energy harvesting. Broad-ranging energy harvesting implementations are discussed, such as vibroacoustic, EM, and thermal energy harvesting schemes.

In contrast with related metasurface energy harvesting surveys [33], [34], this work includes a discussion of metasurface designs for transmitting microwave energy. In addition, it provides an updated treatment of microwave energy harvesting using metasurfaces. The focus is on proposals with a specific potential for deployment in wireless powered networks. In addition, theoretical studies on system-level enhancements derived from the implementation of metasurface-based smart radio environments in wireless powered networks are highlighted. Furthermore, the work highlights current open problems in the practical deployment of metasurfaces in energy transmission and harvesting applications, and suggests possible future research directions.

To this end, the rest of the paper is organized as follows. Section II briefly introduces the features of metasurfaces, while surveys of recent progress in metasurface microwave energy transmission and energy harvesting implementations are presented in Sections III and IV, respectively. Parameters by which the performance of the metasurface structures are characterized are implicit in the presented discussion. Section V reviews studies on the application of metasurfaces as enablers of smart radio environments in next-generation networks supporting information and energy transfer. Open problems in the discussed metasurface implementations are explored in Section VI, with a suggestion of an outlook in the context of wireless powered networks. Section VII concludes the paper.

II. METASURFACE BASICS

Metamaterials are 3D structures with atypical electromagnetic properties, such as near-zero refractive indexes, negative effective permeabilities, and permittivities, which occur at specified frequency bands. These properties enable metamaterials provide unusual functionalities when they interact with EM waves. The effective macro-scale behavior of a metamaterial is realized by positioning sub-wavelength electromagnetic scatterers in regular arrays throughout a given volume of space. Theoretical work by Vesalago [36], and practical demonstrations by Pendry [37] provided the impetus for the wide-ranging interest into metamaterial applications in microwave and optical domains. Recently, there has been an upsurge in interest on 2D metamaterial implementations, known as metasurfaces. One reason for this attention relates to the fact that metasurfaces can be engineered to deliver the required synthetic functionalities using only surface-oriented implementations. Furthermore, metasurfaces are implemented using planar fabrication techniques, which, in general, are less complicated than volumetric fabrication processes used for metamaterials [38].

A metasurface is a thin composite material, comprising of a dielectric substrate upon which a repetitive sub-wavelength pattern of a resonant electromagnetic scatterer, known as the unit cell or meta-atom, is impressed. Although meta-atom patterns are often periodic, aperiodic metasurfaces have also emerged for several applications [39]–[42]. The more common realization of metasurfaces consists of metallic patterns layered on a dielectric substrate. Although single layered metallic meta-cells are often employed, multi-layered implementations have been shown to increase the degrees of freedom in manipulating incident EM waves, leading to enhanced features [43]–[45]. All-dielectric metasurface implementations have also been reported [46]–[49], made possible by the fact that dielectric resonators exhibit geometrically tunable electric and magnetic resonances [43]. Metasurfaces can also be implemented with or without a ground plane beneath the dielectric substrate. When a ground plane is present, the metasurface is also known in the literature as a tensor impedance surface [50], [51].

Metasurfaces are able to realize various manipulations of EM waves, such as non-reciprocal field control, generalized refraction, and polarization transformation [43]. The distribution and geometry of the constituent meta-atoms is critical to the overall response of a metasurface. Generally, the thickness of a metasurface and the dimensions of the meta-atom are small compared to a wavelength in the surrounding media [31]. These sub-wavelength dimensions allow the treatment of metasurfaces as homogenous planar structures. Consequently, the scattering behavior of a metasurface can be characterized using generalized sheet transition conditions (GSTCs) [31], [52], [53].

Although, metasurface design has conventionally relied on optimization-intensive approaches, synthesis techniques have recently emerged, leading to more deterministic methodologies [43], [54]–[56]. A notable technique depends on establishing the tensorial surface electrical and magnetic susceptibility functions of the metasurface on the basis of GSTCs [54]. Then, the physical parameters of the constituent meta-atom are synthesized by mapping the metasurface scattering parameters onto the obtained susceptibility functions, and fine-tuned by optimization [43].

III. METASURFACES FOR MICROWAVE ENERGY TRANSMITTERS

The provision of stable and continuous microwave energy is a crucial consideration in wireless powered networks. As illustrated in Fig. 1, power beacons could be deployed in the network to transmit microwave energy with the specific intent of energizing devices [22], [57]–[60]. There is particular emphasis on the design of transmitting antennas for such microwave energy transmitters. Depending on the network scenario, design requirements could range from having highly directional microwave energy beamed at the intended receiver devices, to having microwave energy beamed over a zone within which devices could receive continuous power.

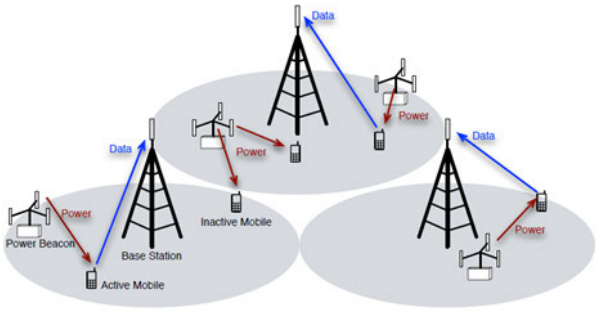

FIGURE 1. Hybrid network overlaying cellular network with randomly deployed power beacons for MPT [21].

In order to support full coverage with minimal interference to existing wireless technologies, it would be necessary to have dense deployments of such power beacons operating at low-power levels in the environment. Such densification would mean that devices are always just a few meters from a microwave energy source, likely within its radiating near-field. From the perspective of the low-power beacon, having the intended receiving devices within this range is advantageous, as it enables focused energy beaming with low attenuation in point-to-point and point-to-multipoint power delivery scenarios [61].

Near-field focused MPT applications have been studied and implemented using antennas [62]–[65]. However, given the unique ability of metasurfaces to tailor wavefronts, it is logical that they have also been studied as a means to realize near-field focusing in optical and radio frequency domains [66]–[69]. Introducing metasurfaces in microwave energy transmission systems potentially provides greater design flexibility, and enhancement of near-field focusing performance, compared to when antennas are used by themselves. Consequently, the following sub-sections focus on recent progress in metasurface research to facilitate focused-beam microwave energy transmission within the radiating near-field.

A. STATIC-BEAM METASURFACES

Static-beam metasurfaces are engineered to focus EM energy at specific spatial coordinates within the radiating near-field of an associated transmitting antenna. As an example, designs of near-field single- and double-focus reflective metasurfaces for microwave energy transmission at 5.8 GHz are presented in [70]. These structures are designed to focus reflected microwave power from a single antenna feed at specific spatial coordinates within the antenna's radiative near-field. While the single-focus design targets point-to-point MPT applications, the double-focus design aims at point-to-multipoint use cases.

In order to ensure good reflective features, the constituent meta-atoms were synthesized as tri-dipoles, as shown in Fig 2. Phase shifts introduced by each tri-dipole element on the incident wave from the feeding antenna collectively constitute the parameter by which various focusing positions are achieved. Since the phase-shift by each tri-dipole is related

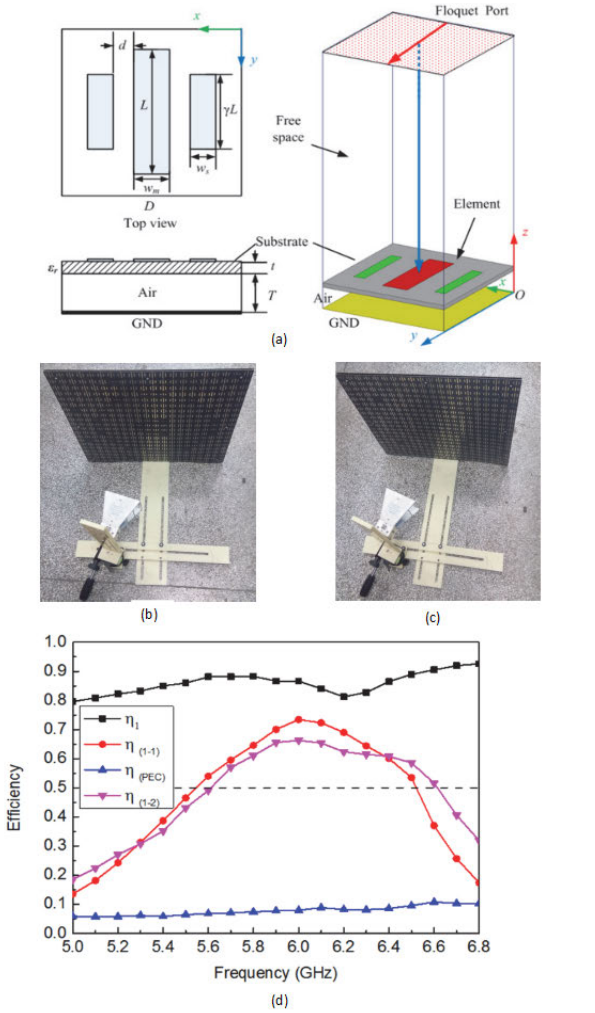

FIGURE 2. Near-field single-focus reflective metasurface (a) Simulation model of tri-dipole meta-atom, (b) single-focus metasurface and feed antenna, (c) double-focus metasurface and antenna. (d) Simulated transfer efficiency curves showing feed-to-metasurface transfer efficiency (η_1); feed-to-single-focus transfer efficiency (η_{1-1}); feed-to-focus transfer efficiency with PEC replacing metasurface (η_{PEC}); and feed-to-double-focus transfer efficiency (η_{1-2}) [70].

to its length, the required phase distributions for the metasurfaces were realized using corresponding distributions of tri-dipole element dimensions. Both metasurfaces had dimensions of 500 mm × 500 mm, and comprised of 20 × 20 elements.

The performance of the metasurface is characterized in terms of a transfer efficiency, which in this case is the percentage ratio of the focused power in the intended direction on the reference plane to the power radiated by the feeding antenna. From the results shown in Fig. 2, it can be seen that at 5.8 GHz the single-focus metasurface design enables the transfer of power from the feed antenna to a desired focal point with a transfer efficiency a little above 60%. Similarly, the double-focus design achieves a slightly lower efficiency level of nearly 60% at the same frequency of interest. For both metasurface designs, the bandwidth at 50% efficiency is about 16%.

In an extension of the methodology introduced in [70], dual-polarized single-focus and dual-focus near-field focusing metasurfaces were introduced in [71]. In order to realize independent control of the incident orthogonal linear polarizations, the elemental meta-atom in both designs were synthesized as a cross-dipole structure, as shown in Fig. 3. Similar to [70], the distribution of phase-shifts required to achieve the focusing position was realized by a corresponding distribution of variation in the sizes of cross-dipole elements across the 390 mm × 390 mm, 26 × 26 element metasurfaces. Synthesized to operate at 10 GHz, the single-focus reflecting metasurface achieved a wireless power transfer efficiency of 71.6% with single polarization excitation. However, with the excitation of both polarizations, the transfer efficiency of the single-focus metasurface dropped to 65.9% at the frequency of interest. On the other hand, the dual-focus design achieved a transfer efficiency of 68.3% at 10 GHz. The relative bandwidths at 50% transfer efficiency for the metasurface designs were approximately 12%, irrespective of the polarization excitation. Measurements also revealed that the inclusion of the single-focus metasurface in the power transmission system led to a 15 dB increase in the wireless power picked up by an intended receiving antenna.

Although metasurfaces are conventionally prototyped using printed-circuit-board (PCB) technology, Yurduseven *et al.* [72] present a polymer metasurface antenna fabricated using 3D printing technology. With the aim of achieving fast low-cost prototyping, the 3D printed metasurface structure was printed in a single-step procedure using polylactic acid and biodegradable Electrifi polymer material, for the dielectric substrate and conductive parts, respectively. Prototypes of the metasurface antenna, shown in Fig. 4, were designed using a holographic beam-focusing technique, leading to different meta-cell iris dimensions and patterns for on-axis and off-axis beam focusing scenarios. As illustrated in Fig. 4, the method works by first establishing a virtual point source **r'** at the position of desired beam focus, which is then back-propagated to the metasurface aperture to provide a desired aperture field distribution **P**. The metasurface **r** is then designed with the objective of producing aperture distribution **P** when excited by the magnetic field **H** of the wave launched by the coaxial feed. In this particular instance, the slot-shaped meta-cells are arranged such that their response to the reference wave is linearly polarized along the vertical axis.

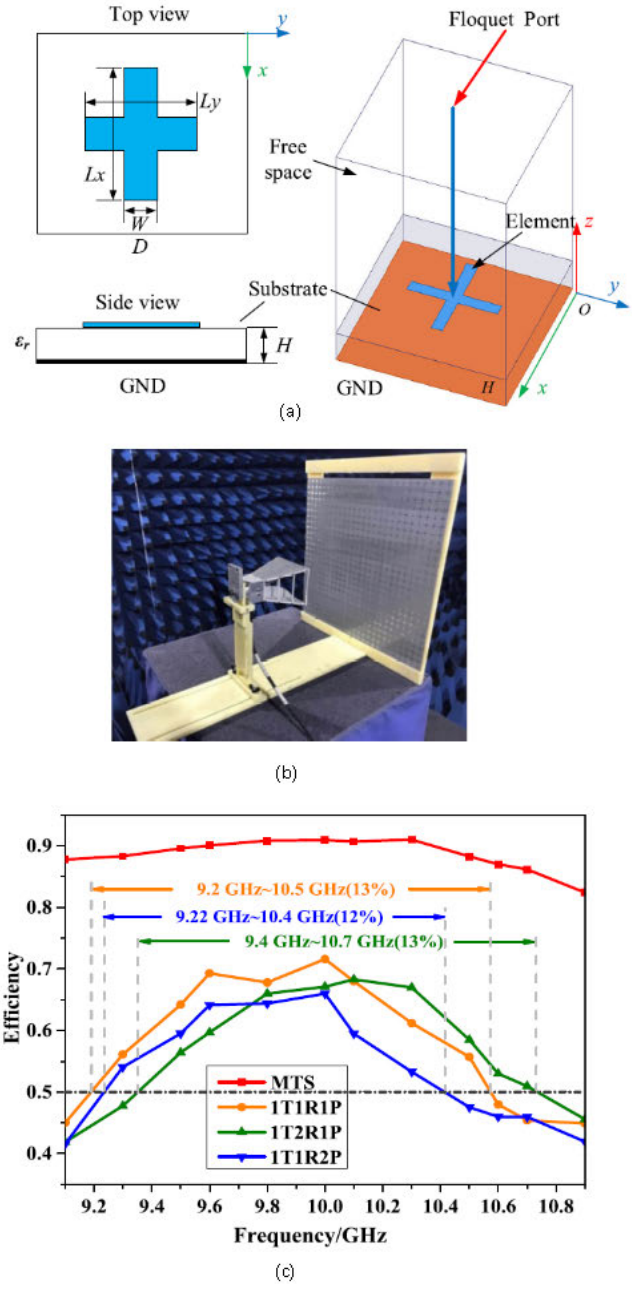

FIGURE 3. Near-field double-focus reflecting metasurface (a) Simulation model of cross-dipole meta-atom, (b) metasurface with feed antenna, (c) Simulated wireless power transfer efficiency curves showing feed-to-metasurface transfer efficiency (MTS); feed-to-single-focus transfer efficiency with single polarization excitation (1TR1P); feed-to-double-focus transfer efficiency with single polarization excitation (1T2R1P); and feed-to-single-focus transfer efficiency with dual polarization excitation (1T1R2P) [71].

B. RECONFIGURABLE METASURFACES

In contrast to previous techniques in which static beam focusing is realized using 'hard-wired' metasurfaces, reconfigurability enables dynamic beam focusing in scenarios were terminals are mobile. Smith *et al.* [25] present a tradeoff analysis of dynamic beam focusing using a conceptual metasurface aperture in a single-focus scenario. The required field phase distribution over the metasurface is holographically determined, by having an assumed point source at the energy receiver location interfere with a plane wave located at the metasurface aperture. In this scenario where the metasurface serves as the microwave radiator itself, the transfer efficiency is characterized as the ratio of the receiver aperture size to the beam waist size at the focus. In a follow up to this initial study, the numerical design of a reconfigurable holographic metasurface aperture for dynamic beam-focusing applications at 20 GHz is presented in [73], [74]. The 150 mm × 150 mm reconfigurable aperture is structured as a parallel-plate

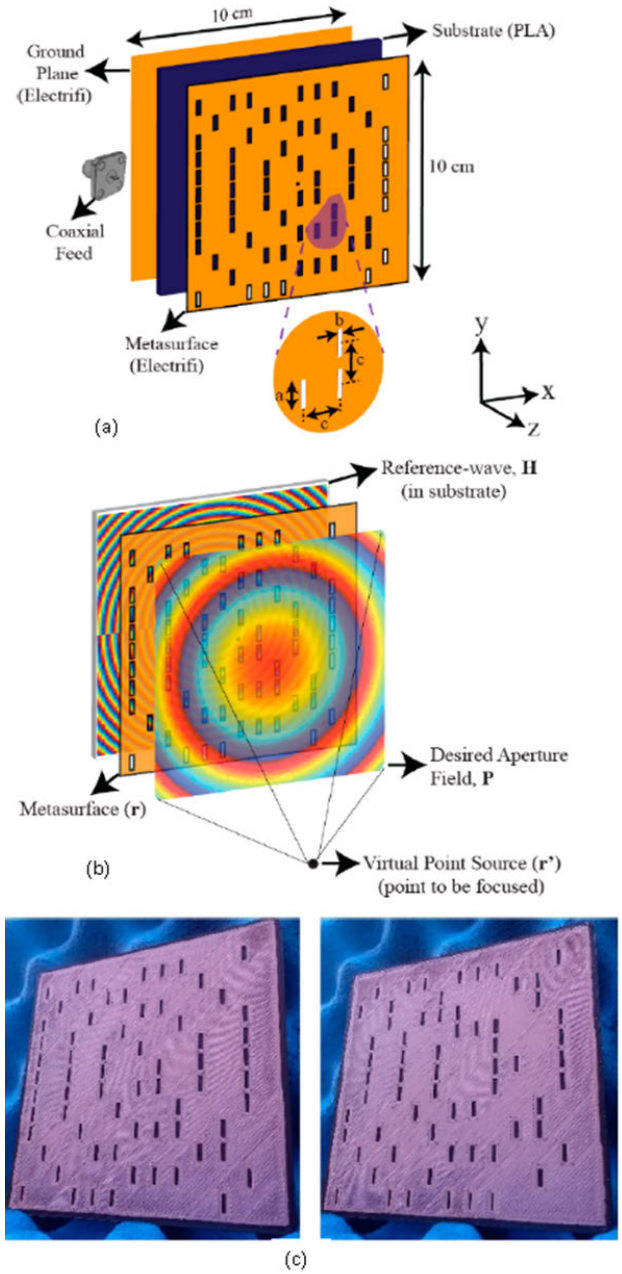

FIGURE 4. Low-cost polymer metasurface (a) metasurface model, (b) illustration of holographic beamforming technique, (c) 3D printed metasurfaces [72].

waveguide, consisting of a dielectric substrate sandwiched between a ground plane and a patterned conducting top plate, as shown in Fig. 5. The meta-atoms on the top plate are slot-shaped irises loaded with PIN diodes. This enables them to be switched between radiating (ON) and non-radiating (OFF) states, depending on the bias applied to the diodes. By this arrangement, the phase distribution of the radiated fields can be reconfigured, thereby enabling beam focusing at any point in the radiative near-field. It is noteworthy that the metasurface aperture in this case serves directly as the beam source, with the excitation for the guided mode launched through a centrally placed coaxial feed.

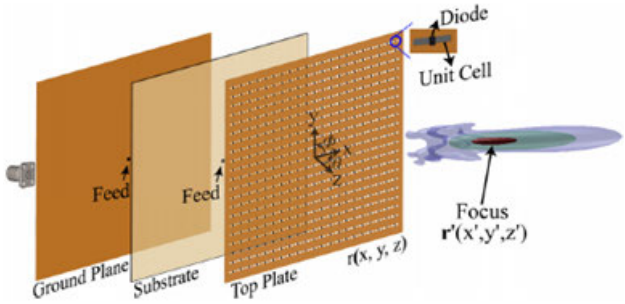

FIGURE 5. Structure of reconfigurable metasurface aperture with centrally placed coaxial feed [73].

Other numerical designs of multi-focus reconfigurable metasurface apertures have been proposed, which leverage the holographic design technique [75], [76]. However, rather than assume a hypothetical point source as a single stationary interferer, multiple mobile energy receivers are the assumed interferers, which are first localized either using a beacon process [75], or a visual binocular location technique [76]. The metasurface apertures are coaxially center-fed, with the meta-atoms patterned as meander line elements, each loaded with three PIN diodes for phase reconfigurability.

The idea of realizing a required beam focusing phase distribution by changing the electrical states of geometrically identical meta-atoms is further extended in Tran *et al.* [77]. Here, a coding metasurface is proposed, where different phase distributions are dynamically realized to manipulate the focal position of an incident beam in response to the motion of an intended receiver. Once again, PIN diodes are used to control the electrical states of individual meta-atoms. In the design, each 1-bit coding meta-atom is capable of operating in either of two states, with codes "1" and "0" mapped onto phase shifts of 0° or 180°, respectively. As shown in Fig. 6, the meta-atom pattern is a fractal structure, etched on a dielectric substrate, with a PIN diode connecting the conductive pattern to the ground plane through a via. A bias line connects the meta-atom to a control board, which provides the required code signaling. The control board implements an adaptive optimal phase control scheme to localize the position of the intended mobile energy receiver, which forms the basis of the control signals for manipulating focal positions of the coding metasurface. The realized 176 mm × 176 mm, 16 × 16 element metasurface was able to dynamically focus the beam from a feed antenna over a range of -60° to 60° in the elevation plane, at 5.8 GHz. The result shown in Fig. 6 reveals that the proposed adaptive optimal phase control scheme enables the metasurface achieve a 4% transfer efficiency at a steering angle of 30°, when measured at a range of 50 cm. It should be noted that, in contrast to [25], the transfer efficiency is here characterized similar to [78], [79] as the ratio of the feed antenna power input to the received power measured at the output of the receiving antenna.

A summary of reviewed research on the use of metasurfaces for near-field focused microwave energy transmission is provided in Table 1.

TABLE 1. Summary of research on metasurfaces for near-field focused microwave power transmission.

Reference, year	Meta-cell structure	Material	Size	Frequency (GHz)	Mode	Focal characteristic	Maximum efficiency (%)
Yu et al. [70], 2019	Tri-dipole	F4B ($\varepsilon_r = 2.65$)	20 x 20 elements, periodicity = 0.48 λ_0^*	5.8	Reflector	Single-focus Dual-focus	 ~60 %
Zhang et al. [71], 2019	Cross-dipole	F4BM-2 ($\varepsilon_r = 2.2$)	26 x 26 element, periodicity = 0.50 λ_0^*	10	Reflector	Single-focus (single polarization) Single-focus (dual polarization) Dual-focus (single polarization)	71.6% 65.9% 68.3%
Yurduseven [72], 2019	Rectangular iris	Polylatic acid ($\varepsilon_r = 3$, tan δ=0.02; Electrifi for conducting layers)	3.33 λ_0^* x 3.33 λ_0^*	10	Transmitter	Single-focus	-
Smith et al. [25], 2017	Iris	-	-	-	Transmitter	-	-
Yurduseven et al. [73], 2017; Yurduseven et al. [74], 2018	Rectangular iris	Rogers 3003 ($\varepsilon_r = 3$, tan δ=0.001)	1.00 λ_0^* x 1.00 λ_0^*	20	Transmitter	Single-focus	-
Luo and Xu [75], 2018	-	-	32 x 32 elements, periodicity = 0.63 λ_0^*	20	Transmitter	Quad-focus	-
Luo [76], 2019	Meander line	-	32 x 32 elements, periodicity = 0.31 λ_0^*	20	Transmitter	Quad-focus	
Tran et al. [77], 2019	Fractal structure	Taconic RF-35 ($\varepsilon_r = 3.5$, tan δ=0.0018)	16 x 16 element, periodicity = 0.21 λ_0^*	5.8	Reflector	Single-focus	~4% at 50 cm distance

* λ_0 is the free-space wavelength at the resonant frequency

IV. METASURFACES FOR MICROWAVE ENERGY HARVESTERS

The primary objective for a microwave energy harvester is to maximally gather microwave energy, which is rectified to provide a stable DC source. As illustrated in Fig. 7, a basic microwave energy harvester requires a collector of EM waves, typically an antenna, to intercept ambient microwave radiation. The AC output of the antenna is rectified to provide a DC voltage, which, after filtering, can be used to drive a connected load. Research on the application of metamaterial elements in microwave energy harvesting has generally proceeded in two directions – as structural enhancements to antennas, or as outright antenna replacements [33]. Motivated by the latter approach, the following sub-sections discuss proposed metasurface antenna substitutes in microwave energy harvesting schemes.

A. META-CELL MICROWAVE ENERGY HARVESTERS

Ramahi *et al.*, in 2012, first demonstrated the ambient EM energy harvesting potentials of meta-cell array structures [80]. The work revealed that individual resonant meta-cells act as energy gatherers when associated with resistive loads, and can collectively facilitate bulk energy gathering when used in array form. The concept was demonstrated by placing a single resistively loaded split-ring resonator (SRR) cell in the direct path of a transmitting array antenna operating at 5.8 GHz. This led to a voltage being observed across the resistor terminals. A similar observation of energy gathering from single SRR meta-cells has been reaffirmed in [81], and detected for an s-shaped meta-cell structure [82], and a ground-backed complementary split-ring resonator (G-CSRR) [83]. However, [80] follows up with a numerical analysis of a 9×9 planar array of SRRs, thereby highlighting a potential for the application of 2D meta-cell arrays as replacements for antennas in microwave energy harvesters. This is further bolstered by the fact that the realized bandwidth is in excess of values usually associated with antenna arrays of similar dimensions. Indeed, vertically stacked 2D SRR arrays have been shown to provide even higher harvesting performance levels [84].

It is equally important to note that [80] proposes a definition for the efficiency of the energy harvester, namely the ratio of the power received by the harvester to the total power incident on the physical area of the harvester. This is the conversion efficiency in the sense that microwave energy incident on the physical harvester is converted to AC power observed at the antenna output port. This efficiency depends on both the frequency and incident angles of the impinging microwave field.

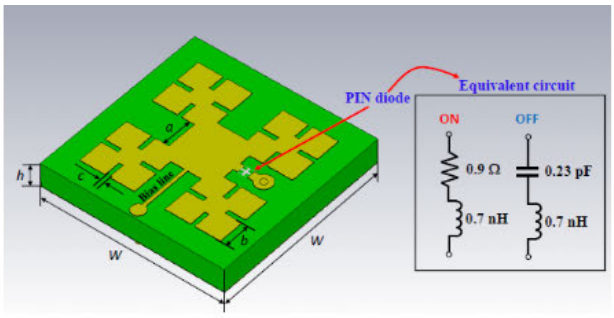

(a)

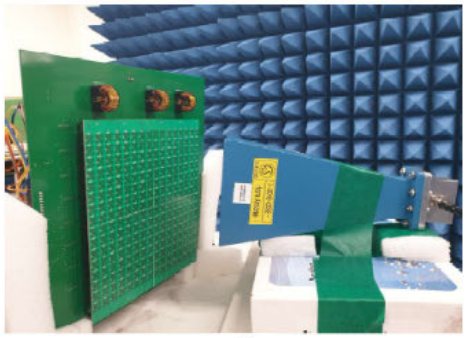

(b)

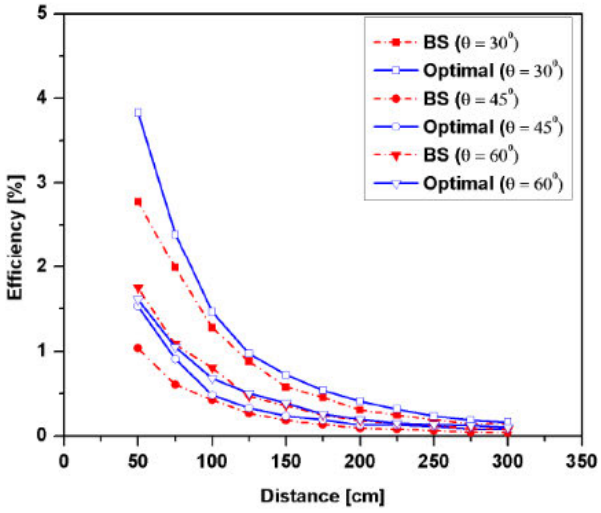

(c)

FIGURE 6. Coding metasurface (a) Fractal meta-atom structure (b) 16 × 16 metasurface with control board under illumination by feed antenna, (c) transfer efficiency using adaptive optimal phase control (Optimal) as compared with a beam synthesis technique (BS) [77].

B. FROM MICROWAVE ENERGY ABSORBERS TO HARVESTERS

Electromagnetic energy absorption is one of the exotic features that can be realized using metamaterial structures. This is made possible by tailoring the material EM response such that incident power is neither reflected nor transmitted [85], [86]. Usually, this requires that the impedance of the metamaterial structure is matched to the free-space impedance. For planar structures, a lossy dielectric substrate and a relatively

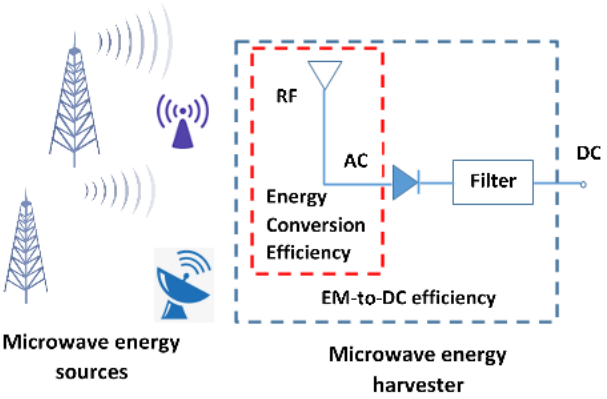

FIGURE 7. Illustration of microwave energy harvesting.

thick ground plane are essential to ensuring that intercepted power is dissipated within the structure, thereby realizing an absorber. In [87], the authors leverage on this principle to design an energy harvesting slab operating at 3 GHz. The design is based on a 2D, 13 × 13 element array of Electric-Inductive-Capacitive (ELC) resonator meta-cells, each connected through a via to a ground-plane-mounted 82 Ω resistor. The resistors were used to mimic the input resistance of a rectifying circuit that could be connected to the port of each meta-cell to extract power. Rather than have the absorbed power dissipated in the lossy dielectric substrate, the design ensured that the greater part of power absorbed by each meta-cell was diverted to its associated resistive load at the resonant frequency. At the operating frequency, simulated and measured conversion efficiencies are 97% and 93%, respectively obtained for the meta-cells. This efficiency level is further enhanced in [88], where the ELC resonators deliver the received energy to a single shared load. The designed 8 × 8 element metasurface (60 mm × 60 mm) achieved a simulated 99.4% conversion efficiency at its resonance frequency of 2.72 GHz.

The energy harvesting potentials of single G-CSRR meta-cells, earlier reported in [83], have been further harnessed by using them in arrays to realize energy harvesting metasurfaces [89]. Simulation results showed that a G-CSRR metasurface conceptualized as an infinite array provided a 92% conversion efficiency, and a 10% half-power bandwidth (HPBW) at a resonance frequency of 5.55 GHz, which are far in excess of the performance of a patch antenna array with the same footprint. The superior performance of the metasurface can be attributed to the higher density of constituent elements that can be achieved without the adverse effects of mutual coupling. For the fabricated 11 × 11 element G-CSRR metasurface, a maximum conversion efficiency of 83% was measured at the central meta-cell. The G-CSRR was also shown to be capable of operating in transmission mode, achieving a calculated radiation efficiency of 93%, which in this case is the ratio of the radiated power to the power available at the input terminal [89].

While it is typical for metasurface harvesters to consist of dielectric substrates sandwiched between two conducting

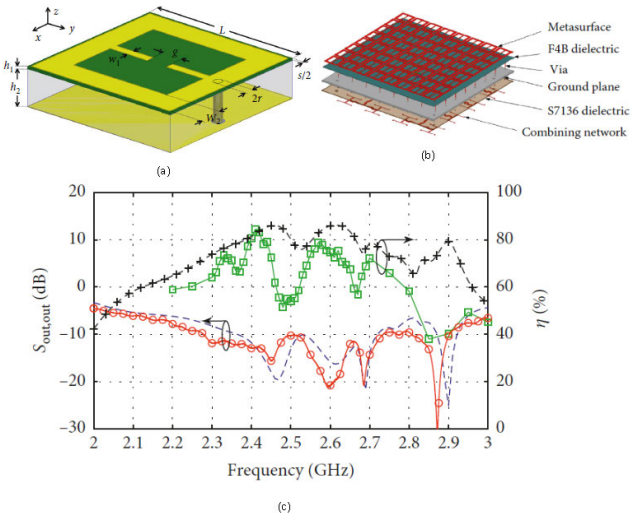

FIGURE 8. Dual-layer metasurface with air-gap (a) ELC meta-cell, (b) 8 × 8 element metasurface, (c) absorption and efficiency results [91].

surfaces, [90], [91] realize the harvester as a dual-layer structure of thin low-loss surfaces separated by an air gap, as illustrated in Fig. 8a.

The air gap provides an additional degree-of-freedom to optimize performance, so that in [91] a 2.2 GHz absorption efficiency of 84.4%, at potentially lower material costs, is obtained. The harvesting metasurface is based on an 8 × 8 element array of ELC resonators on a thin F4B sheet, individually coupled through vias to a combining network loaded on the conducting surface of a ground plane, with both sheets separated by an air gap, as seen in Fig 8.

C. MULTIPLE PERFORMANCE OBJECTIVES

The energy conversion efficiencies realized in [80], [82]–[84], [87]–[91] established the viability of 2D arrays of microwave energy harvesting meta-cells. These implementations can serve as energy collectors in receivers for microwave energy transmission links served by a dedicated wireless source, especially within the radiative near-field. However, for practical far-field energy harvesting, it is important that energy is gathered over a range of frequencies, to enable energy collection from multiple sources. Wider bandwidths roughly correspond to a greater freedom to harvest microwave energy from multiple sources, thereby making the energy harvesting bandwidth an important practical consideration. Consequently, [92] introduces a bandwidth enhancement to the earlier discussed G-CSRR meta-cell structure [89], to realize a metasurface based on an array of wideband G-CSRR (WG-CSRR) meta-cells. The proposed modification is inspired by chaotic bow-tie cavities. Considering that bow-tie structures provide variable reactance, enabling the resonance mechanism of a G-CSRR on a bow-tie inspired pattern provided a meta-cell with resonance over a wide range of frequencies. The simulation results reveal that the WG-CSRR provides similar levels of conversion efficiency to the G-CSRR metasurface [89], but with much larger half-power bandwidth (HPBW). Compared with the 10% HPBW realized in [89], the WG-CSRR achieved a 44% HPBW at its resonance frequency of 5.6 GHz. Moreover, this achieved HPBW performance is 3 times greater than is provided by the ELC array metasurface reported in [87]. Also, similar to [89], the structure can be employed in transmission mode, with a radiation efficiency of 95%.

Complementary to the wideband approach, various multi-band schemes have also been applied to enable microwave energy harvesting over several frequencies. In [93], an SRR-based quad-band metasurface has been designed to harvest microwave energy at the 0.9 GHz, 1.8 GHz, and 2.6 GHz GSM bands, in addition to the 5.8 GHz Wi-Fi band. Numerical analysis of the design revealed an average conversion efficiency of 79.5% over the four bands. A similar quad-band characteristic has also been achieved using a dual-layer meta-cell structure [94].

Corroborating the observation in [80], analysis of the quad-band structure in [93] revealed a significant correlation between the incident angle of impinging fields and the conversion efficiency of the metasurface. This is important because a practical energy harvester is required to simultaneously harvest microwave energy from multiple sources whose spatial locations are unknown a priori. In addition, a practical microwave energy harvester interacts with incident waves of unknown polarizations. It is necessary that metasurface energy harvesters are non-discriminatory towards the diverse polarizations of ambient microwaves. Indeed, the metasurface performance levels reported in [80], [83], [87], [89] are polarization-dependent, which provided an impetus for proposing a metasurface with polarization-independent near-unity conversion efficiency at 2.45 GHz [95].

Recent energy harvesting metasurface designs consequently aim to satisfy multiple performance objectives, such as multi-polarization, wide-angle and multi-frequency characteristics. Polarization-insensitivity, along with triple-band and wide-angle features have been realized using a butterfly-type closed-ring meta-cell (BCR) array [96]. The 7 × 7 element metasurface consist of the array pattern on a low-loss dielectric substrate, with ground backing. Analysis of the metasurface revealed that the structure maintained high efficiency for both transvers electric (TE) and transverse magnetic (TM) oblique incidence at the required resonant frequency bands. Maximum efficiencies of 90%, 83%, and 81% were obtained at the resonance frequencies of 0.9 GHz, 2.7 GHz, and 5.7 GHz, thereby corresponding to the GSM, LTE, and WiFi bands. A similar triple-band, polarization-insensitive, wide-band metasurface is presented in [97], which is targeted at the GSM 1800, WiMax and WiFi bands. Harvesting efficiencies of 30%, 90% and 74% are obtained at 1.75 GHz, 3.8 GHz, and 5.4 GHz. Each cell of the 7 × 7 element array is composed of four identical SRRs arranged in rotational symmetry. Targeting the GSM 900, DCS 1800 and WiFi bands, [98] introduces a tri-band wide-angle harvester based on an array of square-type ELC resonators. Also, a dual-band polarization-insensitive

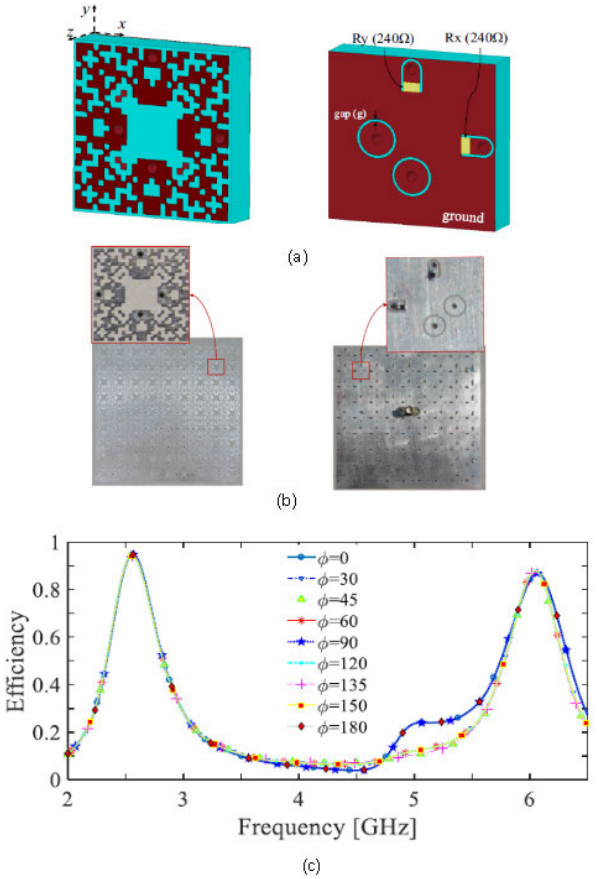

FIGURE 9. Pixelated metasurface (a) pixelated meta-cell with pattern designed using a binary optimization algorithm (front and back view), (b) fabricated metasurface (front and back view), (c) conversion efficiency with different polarizations [99].

implementation at 2.45 GHz and 6 GHz has been realized using a 9 × 9 element array of pixelated meta-cells, shown in Fig. 9 [99]. Alternatively, multi-frequency response can be realized through wideband structures. An example is the 5 × 5 element wideband metasurface using meta-cells, each comprising of a square ring and four metal bars [100]. For a randomly polarized wave at perpendicular incidence, the structure provided a HPBW level of 110% and 96% efficiency. With an increase of the incident angle to 45°, the metasurface still provided efficiency levels beyond 88%, and HPBW greater than 83%.

Some designs have placed more emphasis on polarization-insensitivity and wide-angle incidence. One such example is a 5 × 5 element metasurface operating at 5.8 GHz [101]. Similarly, high energy harvesting efficiency, wide-angle incidence and polarization-insensitivity has been achieved using a 9 × 9 square-ring resonator element metasurface at 2.5 GHz [102], shown in Fig. 10. Also, while wide-angle polarization-independent energy harvesting at 2.45 GHz has been studied using a fractal meta-cell [103], a novel ELC meta-cell [104] has been investigated for polarization-independent energy harvesting at the same frequency. A different study provides a dual-band polarization-independent wide-angle metasurface,

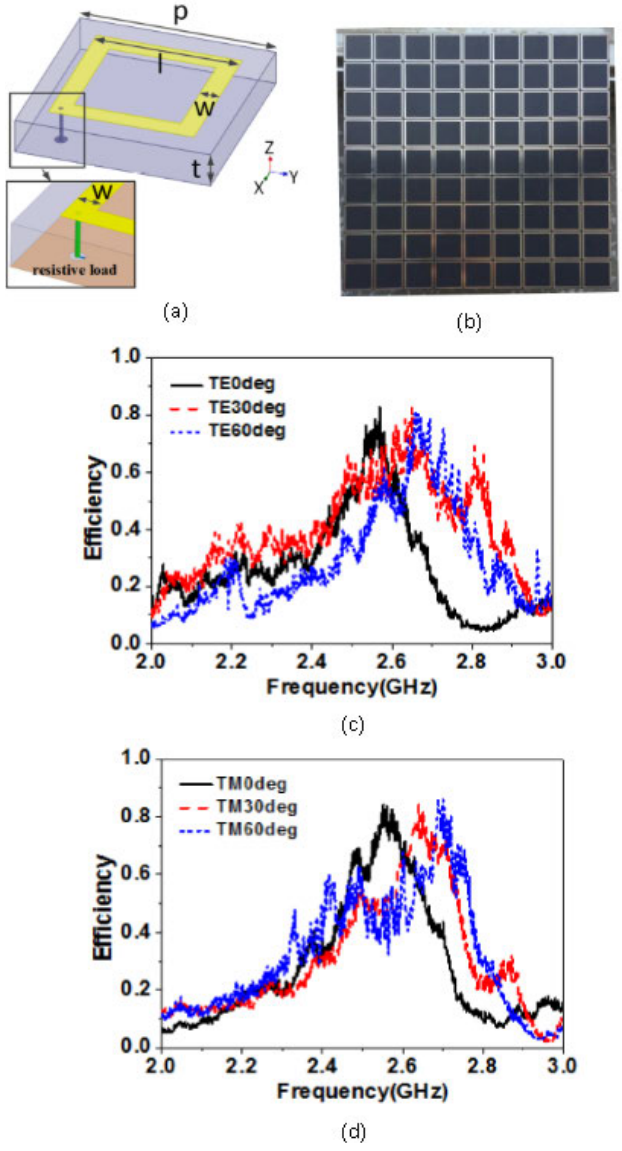

FIGURE 10. Wide-angle and polarization-insensitive metasurface (a) square-ring resonator meta-cell, (b) fabricated metasurface, (c) conversion efficiencies with TE polarization, (d) conversion efficiencies with TM polarization [102].

simulated as an infinite array of closed ring resonators [105]. High efficiencies are maintained with oblique incident angles at either TE or TM polarization, with maximum efficiencies of 91% and 84% realized at 2.7 GHz and 5 GHz, respectively. Similarly, the design reported in [106] achieves polarization-insensitivity and stable frequency response over a wide range of incidence angles. The structure, shown in Fig. 11, achieves a 91% conversion efficiency at 5.8 GHz for both TE and TM polarizations with normal incidence. Also a 0.19% shift in resonance frequency is observed when the incidence angle is increased to 75°. In contrast, however, [107] is silent on the polarization independence of the proposed structure, preferring rather to optimize wideband and wide incident angle characteristics of the metasurface. The proposed 10 × 10 element structure, shown in Fig. 12, yields a 16% relative

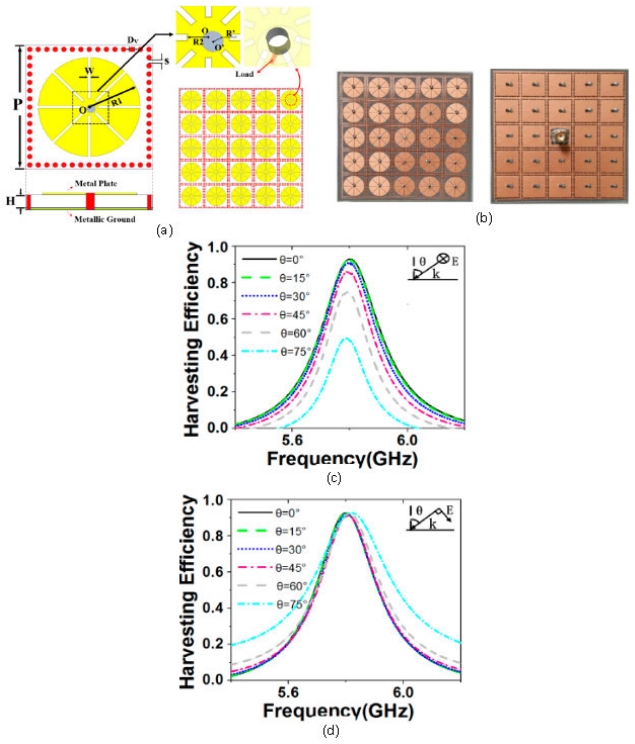

FIGURE 11. Polarization-insensitive wide-angle metasurface (a) meta-cell model surrounded by square pattern of vias (in red), (b) fabricated 5 × 5 element metasurface, (c) conversion efficiencies with TE polarization (d) conversion efficiencies with TM polarization [106].

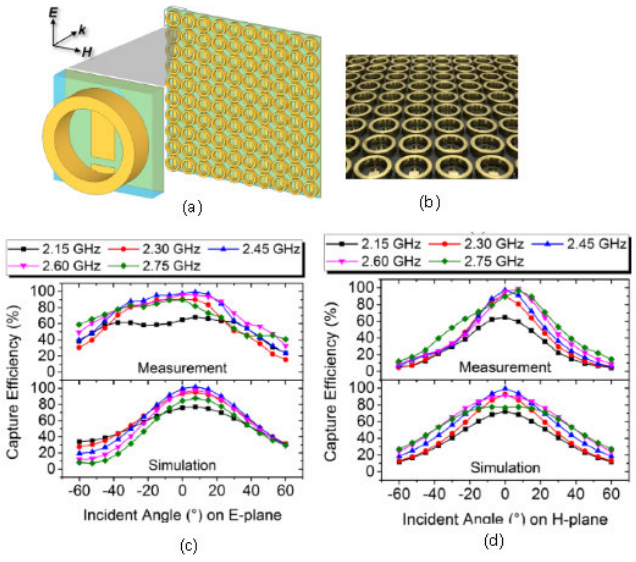

FIGURE 12. Wideband, wide-angle metasurface (a) meta-cell and metasurface models, (b) fabricated metasurface, (c) incident angles on E-plane, (d) incident angles on H-plane [107].

bandwidth, with 92° and 44° angle ranges in the E- and H-planes, respectively.

D. FLEXIBLE MATERIALS

There have been attempts to implement energy harvesting metasurfaces using flexible materials, rather than conventional mechanically rigid structures. A flexible metasurface,

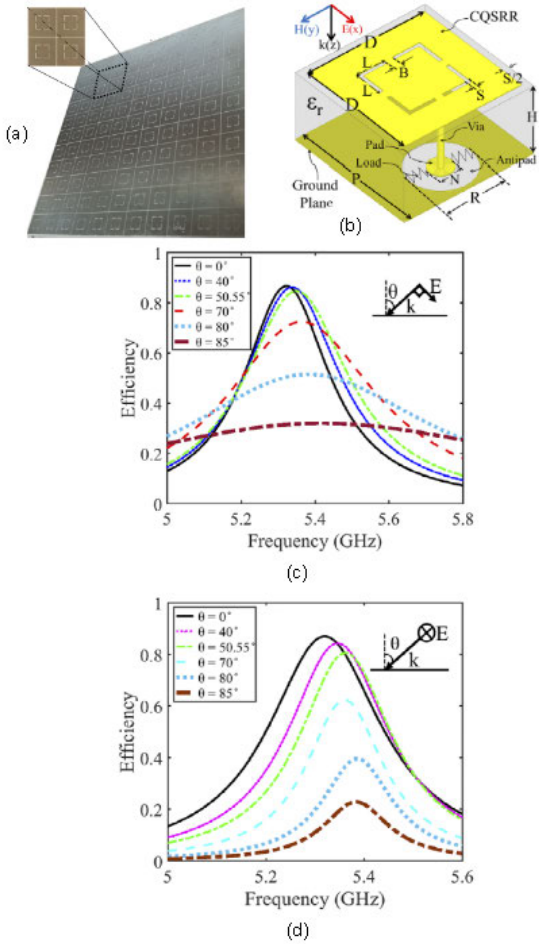

FIGURE 13. Flexible metasurface (a) fabricated metasurface, (b) CQSRR meta-cell model, (c) simulated conversion efficiency with incidence angles on H-plane (d) simulated conversion efficiency with incidence angles on E-plane [108].

shown in Fig. 13, has been realized using a complementary quad split ring resonator (CQSRR) meta-cell pattern printed on a ground-backed Rogers 3010 substrate, with a thickness of 0.254 mm [108]. The thinness of the substrate allows for a bending of the 11 × 11 element metasurface over a radius of 48 mm, while still maintaining high efficiency levels at oblique incident angles. Similarly, a dual-band metasurface harvester, shown in Fig. 14, has been designed for operation at 10.1 GHz and 42.86 GHz. The structure provides more than 70% conversion efficiency over 170° (i.e. 2 × 85°) incident angle of TM-polarized waves at the lower resonance frequency of 10.1 GHz [109].

E. RECTIFYING METASURFACES

Apart from metasurfaces being used as antenna replacements in energy harvesters, they have also been conceptualized as outright replacements for the antenna-rectifier stage – the rectenna, often designed as a single unit [110], [111]. Consequently, with the notion that, as standalone units, DC voltages should be directly obtained at metasurface output ports, some research has focused on implementing both microwave

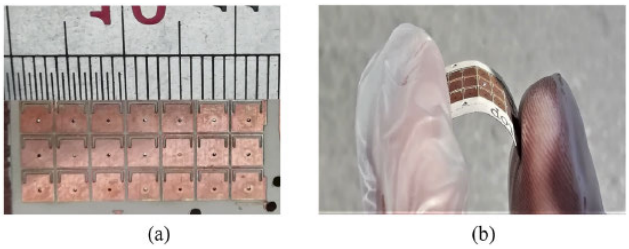

FIGURE 14. Prototype of ultra-thin flexible 3 × 7 element dual-band metasurface harvester (a) illustration of small size, (b) illustration of metasurface flexibility [109].

energy collection and rectification on the metasurface structure itself.

Hawkes *et al.* [112] first experimentally demonstrated the rectifying metasurface concept, using a Greinacher rectifier circuit within an SRR operating at 900 MHz [112]. Subsequent research has sought to maximize the EM-to-DC efficiency of rectifying metasurface structures. One such design endeavor realized an EM-to-DC efficiency of 35.1% [113]. In another design, an EM-to-DC efficiency above 40% at 3 GHz was obtained using an 8 × 8 2D array of cross resonators, which is connected through a corporate feed network to a ground-mounted rectifier circuit, as shown in Fig. 15 [114]. The realized EM-to-DC efficiency level was subsequently improved to slightly more than 55% at 2.72 GHz, with ELC resonator elements substituted for the cross resonator meta-cells [115]. A further enhancement is reported in [116], where a maximum EM-to-DC efficiency of 75% was obtained at an incident 2.45 GHz power level of 0.4 dBm. As shown in Fig. 16, each meta-cell is realized as a top-layer ELC structure coupled to a voltage-doubler rectifier implemented on the ground plane. An alternative implementation of a 2.45 GHz rectifying metasurface is a 3-layer structure based on a 6 × 6 element array of mirrored split rings, a ground plane, and a layer accommodating Schottky diode rectifiers, yielding a measured conversion efficiency of 44.5% at a 5 mW/cm^2 incident power density [117]. An optimized design of this structure, shown in Fig. 17, yielded a measured harvesting efficiency of 66.9 % with the same incident power density [118]. In another example, a dual-polarized wide-angle rectifying metasurface based on a 3 × 3 array of super cells, shown in Fig. 18, has been presented for energy harvesting at 2.4 GHz [119]. With the structure able to provide conversion and AC-to-DC efficiencies of 90% and 80%, respectively, EM-to-DC efficiencies up to 72% are consequently implied. Each super-cell structure is a 4 × 4 array of ELC resonators on top of a dielectric substrate, backed by a ground plane that hosts the feeding network and rectifying circuit. Likewise, an 8 × 8 element metasurface, based on face-to-face split SRR cells, which is shown in Fig. 19, has been employed to provide an EM-to-DC efficiency 67% [120].

A purely coplanar rectifying metasurface structure, which has less complex implementation requirements, is reported in [121]. The work proposes embedding a PN junction

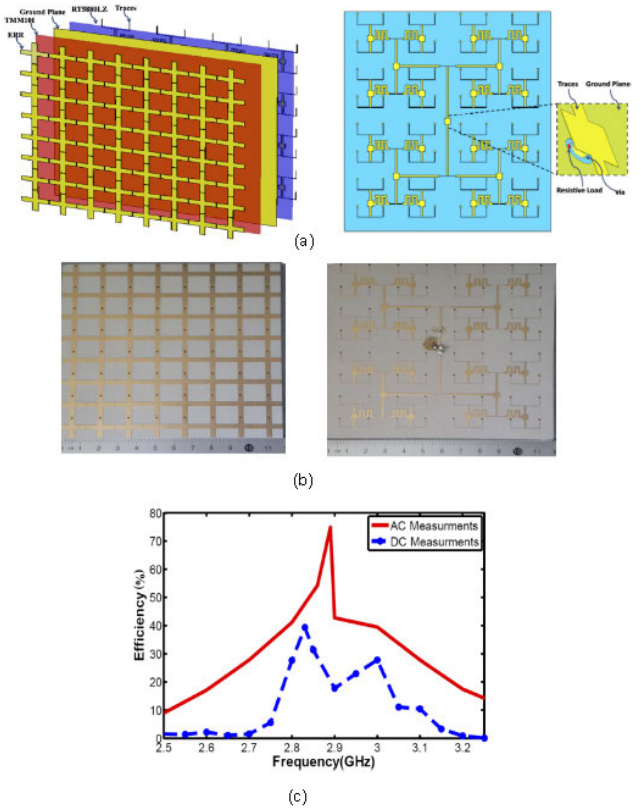

FIGURE 15. 8 × 8 element cross resonator element metasurface (a) Model of rectifying metasurface showing different layers, and rectifying circuit at bottom layer, (b) fabricated metasurface, top and bottom views, (c) measured conversion and EM-to-DC efficiencies [114].

diode directly within each cut-wire meta-cell. The resonant meta-cell structure with an integrated diode resonates approximately at 6.75 GHz. However, the harvesting efficiency is shown to be dependent on the diode technology, with a 50% conversion efficiency obtained using germanium diodes. With a similar motivation for planar implementations, [122] presents a numerical analysis of a dual polarized metasurface harvester, where the rectifying diodes can be placed directly at the feed point of constituent meta-cells. The analysis examines the performance of an 8 × 8 element metasurface, where each 2×2 element block constitutes a super-cell structure able to resonate to orthogonal polarizations at 2 GHz. As shown in Fig. 20, the structure achieves 98 % conversion efficiency, and 58% EM-to-DC efficiency.

More recently, a miniaturized dual-band rectifying metasurface, with polarization independence and wide-angle incidence has been developed [123]. The compact, single-layered structure is realized through surface-mount technology, with the elimination of an impedance matching network between the metasurface and the rectification stage. The design is able to capture waves of arbitrary polarizations over an angle range of 60°. In addition, measurements conducted at an input power level of 0 dB, with different incident angles and polarizations on a 4×4 element prototype, provide maximum EM-to-DC efficiencies of 58% and 50%, at 2.4 GHz and 5.8 GHz, respectively. Critically, the design is also shown to

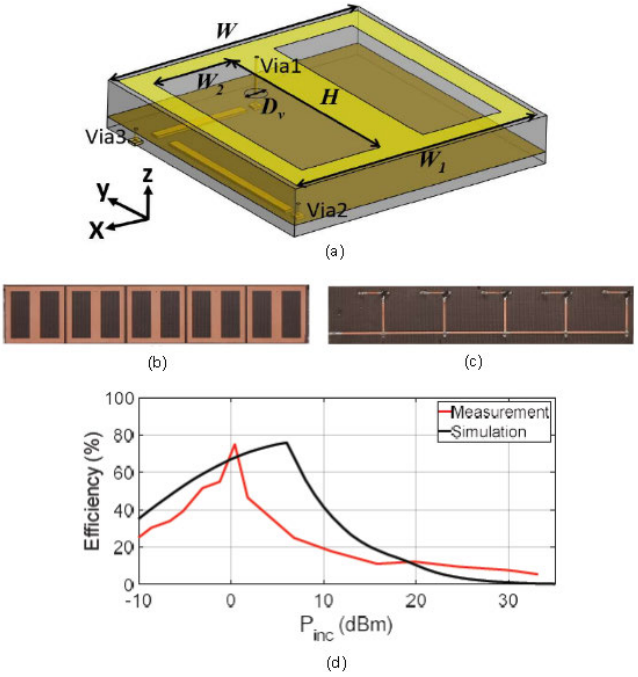

FIGURE 16. Rectifying metasurface (a) ELC meta-cell model, (b) fabricated 1 × 5 element rectifying metasurface, top view, (c) fabricated 1 × 5 element rectifying metasurface, bottom view, (d) EM-to-DC efficiency vs input power at 2.45 GHz with 300Ω load [116].

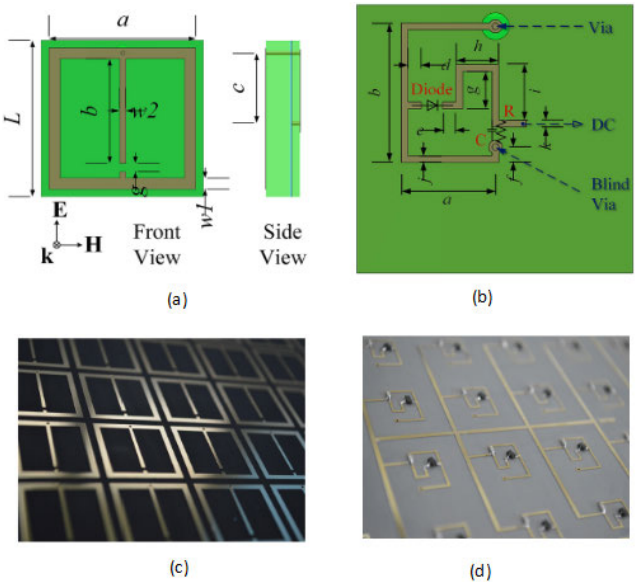

FIGURE 17. Rectifying metasurface (a) mirrored SRR meta-cell model, (b) back view of meta-cell showing Schottky diode rectifier (c) 6 × 6 element rectifying metasurface, top-view, (d) bottom-view of fabricated metasurface [118].

have a flexible input power requirement, maintaining high efficiency levels over an input power range from −3dBm to 10 dBm.

The reviewed research on metasurface implementations of microwave energy harvesters is summarized in Table 2.

V. POWERING SMART RADIO ENVIRONMENTS AND NEXT-GENERATION WIRELESS NETWORKS

Besides the promise of greater data rates, future 6G wireless networks are envisaged to enable smart living, through the provision of pervasive information processing capabilities and context-awareness, beyond the current performance limits of wireless technologies [1]. In order to overcome present fundamental wireless limitations, smart radio environments are being proposed as key features of next-generation wireless networks [1], [124]–[128]. This is a radically different concept from the conventional formulation of the radio channel as an uncontrollable and adversarial entity. Rather, through the introduction of specially engineered programmable objects into the ambient environment between transmitters and receivers, the radio channel is effectively transformed into a programmable space, which can be controlled and optimized.

The seminal paper by Renzo *et al* [124] provides an in-depth discussion of reconfigurable intelligent surfaces (RISs) as key enablers for the implementation of smart radio environments in next-generation wireless networks. The paper notes that RISs can be realized by integrating active control devices, communication interfaces, and sensing capabilities onto metasurface structures. Such RIS implementations can be regarded as nearly-passive, with minimal power and signal processing required during the configuration phase. This opens up opportunities for a new class of multi-functional software-controlled metasurfaces, where energy harvesting is a pre-requisite functionality to energize the smart surface for other signal processing, sensing and communication tasks. As noted in [124], there are a number of ongoing collaborative projects in this regard [129], [130].

There are a number of theoretical investigations of system performance gains arising from the deployment of RISs in various network scenarios supporting simultaneous wireless information and power transfer (SWIPT) in a wireless network. Downlink multi-user multiple-input single-output (MISO) scenarios, for example, have been examined in a number of works. Huang *et al* [131] provides a power consumption model for a downlink MISO system assisted by an RIS, which factors the RIS power dissipation into the overall power budget of the link. Noting that signal forwarding by an RIS is achieved without amplifiers, the presented analysis reveals the attainment of significantly higher system energy efficiencies compared to the use of multi-antenna amplify-and-forward (AF) relays. Similarly, in [132], the scenario is one in which a multi-antenna access point employs transmit beamforming to send information and energy signals to a set of information and energy harvesting receivers. The work maximizes the minimum power received by the energy receivers by jointly optimizing the information and energy transmit beamforming, along with the reflective beamforming at the introduced RIS. The presented analysis reveals that RIS-assisted SWIPT schemes are significantly enhanced compared to other reference systems without RIS deployments. In [133], the authors investigate a system in which multiple RISs assist in information and power transfer

TABLE 2. Summary of microwave energy harvesting metasurface designs.

References, (year)	Meta-cell Structure	Material	Metasurface size	Frequency (GHz)	Max efficiency (%) Conversion	EM-to-DC	Key point
Ramahi et al. [80], 2012	SRR	Rogers Duroid RT5880 (ε_r = 3, tan δ=0.02;	9 x 9 element, periodicity = 0.18 λ_0^*	5.8	76	-	Establishes harvesting potential of 2D meta-cell arrays.
Almoneef and Ramahi [87], 2015	ELC	Rogers TMM10i (ε_r = 9.9, tan δ=0.002)	13 x 13 element, periodicity = 0.07 λ_0^*	3	97	-	Near unity efficiency.
El Badawe and Ramahi [88], 2016	ELC	Rogers RT6006 (ε_r = 6.15, tan δ=0.0027)	8 x 8 element, periodicity = 0.07 λ_0^*	2.72	99.4	-	Shared load between meta-cells.
Alavikia et al. [88], 2015	G-CSRR	Rogers Duroid RT5880	11 x 11 element, periodicity = 0.34 λ_0^*	5.55	92	-	93% radiation efficiency in transmission mode.
Hu et al., [89], 2018, [91] 2019	ELC	Rogers RT Duroid 5880 (ε_r = 2.2, tan δ=0.001)	8 x 8 element, periodicity = 0.17 λ_0^*	2.41	84.4	-	Dual-layer structure with thin low-loss material and air-gap.
Alavikia et al. [92], 2015	WG-CSRR	Rogers RO4003	9 x 9 element, periodicity = 0.20 λ_0^*	5.6	~ 87	-	95% radiation efficiency in transmission mode at 5.48 GHz.
Karakaya et al. [93], 2019	4 Nested SRRs	Polytetrafluoroethylene, (ε_r = 2.1, tan δ=0.0002)	4 x 6 element, period = 43.00 mm	0.90, 1.80, 2.60, 5.80	85.7, 82.0, 80.4, 69.8	-	Quad-band harvester.
Ghaderi et al. [95], 2018	ELC	Rogers RT Duroid 6006 (ε_r = 6.15, tan δ=0.0027)	9 x 9 element, periodicity = 0.09 λ_0^*	2.45	> 92	-	Polarization-insensitive.
Zhang et al. [96], 2017	BCR	F4B (ε_r = 2.65, tan δ=0.001)	7 x 7 element, period = 26.90 mm	0.9, 2.9, 5.7	90, 83, 81	-	Triple-band, wide-angle incident and polarization-insensitive.
Zhong et al. [97]. 2016	4 SRRs in rotating symmetry	Rogers RO4003 (ε_r = 3.38, tan δ=0.0027)	7 x 7 element, period = 31.65 mm	1.75, 3.8. 5.4	30, 90, 74	-	Triple-band, wide-angle incident and polarization-insensitive.
Assimonis et al. [98], 2016	ELC	Foam (ε_r = 1.04, tan δ=0.001)	Infinite array, period = 33.31 mm	0.9, 1.8, 2.45	94, 81, 87	-	Triple-band, wide-angle incident.
Ghaderi et al. [99], 2018	Pixelated resonator	Rogers RT Duroid 6006 (ε_r = 6.15, tan δ=0.0027)	9 x 9 element, period = 11.40 mm	2.45, 6	95, 90	-	Dual-band, polarization-insensitive.
Zhong et al. [100], 2017	Square ring and 4 metal bars	F4B-2 (ε_r = 2.65, tan δ=0.001)	48 mm x 48 mm, 5 x 5 element, period = 9.6 mm	HPBW = 6.2 – 20.7	96	-	Wideband, wide-angle incident and polarization-insensitive.

from a multi-antenna access point to multiple single-antenna users, with an aim to minimizing the access point transmit power. Conventional alternating optimization is shown to be inefficient in tackling the resulting non-convex problem as formulated, and a penalty-based algorithm is proffered as an alternative, Also, a MISO WPT system where the transmitter

TABLE 2. *(Continued.)* **Summary of microwave energy harvesting metasurface designs.**

Yu et al. [101], 2018	Proprietary shape	Unknown (ε_r = 2.2, tan δ=0.001)	5 x 5 element, periodicity = 0.32 λ_0^*	5.8	88	-	Wide-angle incident and polarization-insensitive.
Zhang et al. [102], 2018	Square ring	F4B (ε_r = 2.65, tan δ=0.001)	9 x 9 element, periodicity = 0.13 λ_0^*	2.5	>80	-	Wide-angle incident and polarization-insensitive.
Costanzo and Venneri [103], 2020	Minkowski fractal	Rogers TMM10i (ε_r = 9.8, tan δ=0.002)	9 x 9 element, periodicity = 0.12 λ_0^*	2.45	96.5	-	Wide-angle incident and polarization-insensitive.
Ghaderi, et al. [104], 2018	ELC	Rogers RT Duroid 6006 (ε_r = 6.15, tan δ=0.0027)	9 x 9 element, periodicity = 0.09 λ_0^*	2.45	>92%	-	Polarization-insensitive
Zhang and Li [105], 2017	Square closed-ring	FB4	Infinite array, period = 20.00 mm	2.7, 5	91.1, 85	-	Dual-band, wide-angle incident and polarization-insensitive.
Yu, et al. [106], 2020	Symmetrical circular sectors, surrounded by square pattern of metal vias.	Unknown (ε_r = 2.65, tan δ=0.0012)	5 x 5 element, periodicity = 0.29 λ_0^*	5.8	91	-	Frequency stability with wide-angle incidence, and polarization-insensitive
Duan et al. [107], 2018	Mirrored split rings and hollow cylinders	Polytetrafluoroethylene (ε_r = 2.65, tan δ=0.0007)	10 x 10 element, periodicity = 0.16 λ_0^*	2.45	97.3%	-	Wideband, wide-angle incident.
Ghaneizadeh et al. [108], 2019	CQSRR	Rogers RO3010 (ε_r = 10.2, tan δ=0.0022)	11 x 11 element periodicity = 0.14 λ_0^*	5.33	86	-	Flexible and ultra-thin.
Ghaneizadeh et al. [109], 2020	C-shaped slot	Rogers RO3010 (ε_r = 11.2, tan δ=0.0022)	7 x 3 element, period = 3.27 mm	10.1, 42.86	93.4, 84.3	-	Dual-band, flexible and ultra-thin. Wide-angle incidence at lower frequency.
Zhao et al. [113], 2018	CSRR	F4B (ε_r = 2.65, tan δ=0.001)	4 x 4 element, periodicity = 0.31 λ_0^*	5.16	98.9%	35.1% at -10dB incident power	Rectifying metasurface.
El Badawe et al. [114], 2017	Cross resonators	Meta-cells: Rogers TMM10I (ε_r = 9.9, tan δ=0.002) Feed network: Rogers RT5880LZ (ε_r = 1.96, tan δ=0.0019)	8 x 8 element, periodicity = 0.15 λ_0^*	3	92	40 at 12dBm incident power.	Rectifying metasurface.
El Badawe and Ramahi [115], 2018	ELC	Rogers RT6006 (ε_r = 6.15, tan δ=0.0027)	60 mm x 60 mm 8 x 8 element, periodicity = 0.07 λ_0^*	2.72	99	>55 at -2 dBm incident power	Rectifying metasurface.
Lee and Hong [116], 2020	ELC	Meta-cells: TACONIC TLX-8 (ε_r = 2.55) Rectifier circuit:	1 x 5 element, periodicity = 0.06 λ_0^*	2.45	-	75 at 0.4 dBm	Rectifying metasurface.

TABLE 2. ***(Continued.)*** **Summary of microwave energy harvesting metasurface designs.**

		TACONIC TLX-9 (ε_r = 2.5) Bonding layer: TACONIC TacBond HT 1.5 (ε_r = 2.35)					
Duan et al. [117], 2016	ELC	Rogers RO4450F	6 x 6 element, periodicity = 0.16 λ_0*	2.45	-	44.5 at 5 mW/cm^2	Rectifying metasurface
Duan et al. [118], 2016	Mirrored split-rings	Polytetrafluoroethylene (ε_r = 2.65, tan δ=0.0007)	6 x 6 element, periodicity = 0.16 λ_0*	2.45	-	66.9 at mW/cm^2	Rectifying metasurface
Almoneef et al. [119], 2017	4 x 4 ELC super cell	Rogers RT Duroid 5880 (ε_r = 2.2, tan δ=0.0009)	3 x 3 (super cell) element, periodicity = 0.56 λ_0*	2.4	~90	~72 at 9 dBm	Polarization-insensitive rectifying metasurface
Xu et al. [120], 2016	Face-to-face SRR	Rogers 04350 (ε_r = 3.48, tan δ=0.0037)	8 x 8 element periodicity = 0.13 λ_0*	2.45	86	67 at 10 dBm	Rectifying metasurface.
Tekam et al. [121], 2017	Cut-wire	-	5 x 5 element, periodicity = 0.67 λ_0*	6.75	-	50 at 1.13 W/m^2	Rectifying metasurface, co-planar implementation.
Aldhaeebi and Almoneef [122], 2020	Circular loop with embedded dipole	Rogers RO4003C (ε_r = 3.38, tan δ=0.0027)	8 x 8 element, periodicity = 0.13 λ_0*	2	98%	58%	Dual-polarized rectifying metasurface
Li et al. [123], 2020	Square metal pad with four pairs of connecting branches	Rogers 3210 (ε_r = 10.2, tan δ=0.0027)	4 x 4 element, period = 16 mm	2.4, 5.8	92%, 88%	58%, 50%, both at 0 dBm	Dual-band, polarization insensitive, wide-angle incident, planar implementation, without matching network

* λ_0 is the free-space wavelength at the resonant frequency

has a constant envelope analog beamformer has been studied in [134]. The performance gains derived from employing RISs are revealed when the transmitter beamformer and the RIS phase shifts are jointly optimized, subject to minimal received power constraints of users.

Secure information and power transfer in RIS-enabled links has also received research attention. In [135], the focus is on maximizing the harvested energy in a MISO system under secrecy rate and RIS reflecting phase shift constraints. This is achieved by jointly optimizing the secure access point transmit beamforming and the RIS phase shifts through a proposed successive convex approximation technique. The obtained numerical results reveal a doubling of the harvested energy as a consequence of the introduced RIS. On the other hand, the authors in [136] investigate a scenario in which the energy receiver in a SWIPT system is a potential eavesdropper. Using an inexact block coordinate descent (IBCD) method, the secrecy rate is maximized through a joint design of the precoding matrix, the artificial noise covariance, and the phase shift matrix, subject to the harvested energy and unit modulus reflect coefficient constraints.

An important issue in SWIPT systems is the rate-energy trade-off performance, which is influenced by differences in power levels required by information decoders and energy receivers. In [137], the authors consider the case of an RIS deployed to assist a multi-antenna access point serving multiple information decoders and energy receivers. By proposing efficient algorithms to obtain suboptimal solutions for the joint optimization of access point precoding and RIS phase shifts, the work reveals that information signals alone are sufficient to serve both information and energy receivers with arbitrary user channels. Furthermore, an RIS in strong line-of-sight with the access point is shown to improve the energy harvesting performance of energy receivers. On the other hand, Zhao *et al* [138] maximizes the rate-energy trade-off in an RIS-aided system, with a multi-antenna access point that transmits information and energy signals to a single user. This is achieved through a joint optimization of the

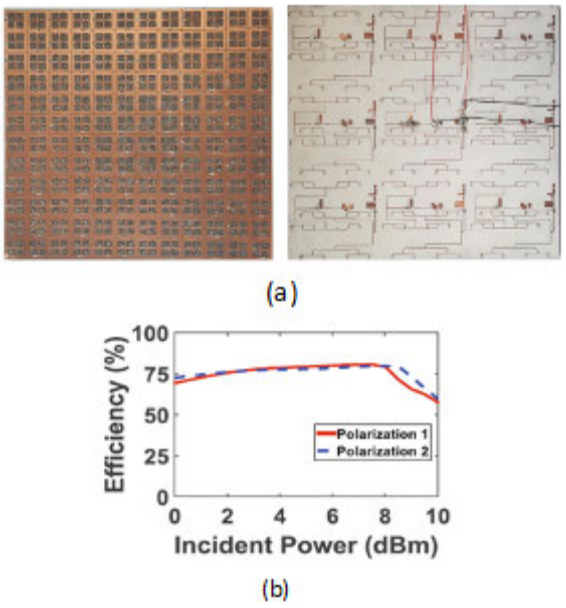

FIGURE 18. Dual-polarized, wide-angle metasurface (a) top and bottom views of 3 × 3 super-cell rectifying metasurface, where each super-cell is a 4 × 4 element unit, leading to a total of 144 meta-cells (b) EM-to-DC efficiency at 2.4 GHz [119].

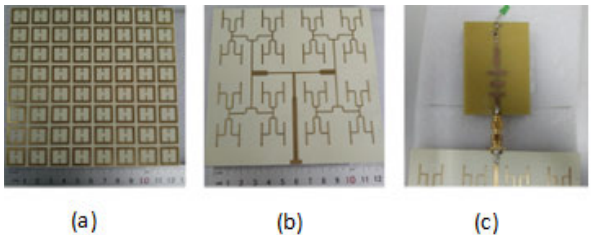

FIGURE 19. 8 × 8 element rectifying metasurface (a) SRR pattern on top layer, (b) feed network at bottom layer, (c) single rectifier attached to metasurface structure.

transmit waveform and beamforming at the access point; the reflection coefficient at the RIS; and the power splitting ratio for information decoding and energy harvesting at the user. In this scenario, the authors assert that energy harvester non-linearities impose a requirement for a dedicated energy waveform to boost the rate-energy performance trade-off.

Other areas that have been examined include user cooperation [139], and multiple-input multiple-output (MIMO) SWIPT scenarios [140]. The scenario in [139], involves two users harvesting wireless energy and transmitting information to a shared hybrid access point. Here, the authors tackled the combined throughput maximization problem using a joint optimization of the RIS phase shifts, the transmission time and power allocations. The obtained results verified the efficacy of RISs in improving the throughput of cooperative transmissions in wireless powered communication networks. On the other hand, Pan *et al.* [140] analyze a MIMO broadcast SWIPT system, where an RIS is used to enhance the energy harvesting capabilities of the network. The investigated scenario consists of a multi-antenna base station communicating with several multi-antenna receivers, with guaranteed energy harvesting requirements. Through the application of the block coordinate descent (BCD) algorithm, the numerical results

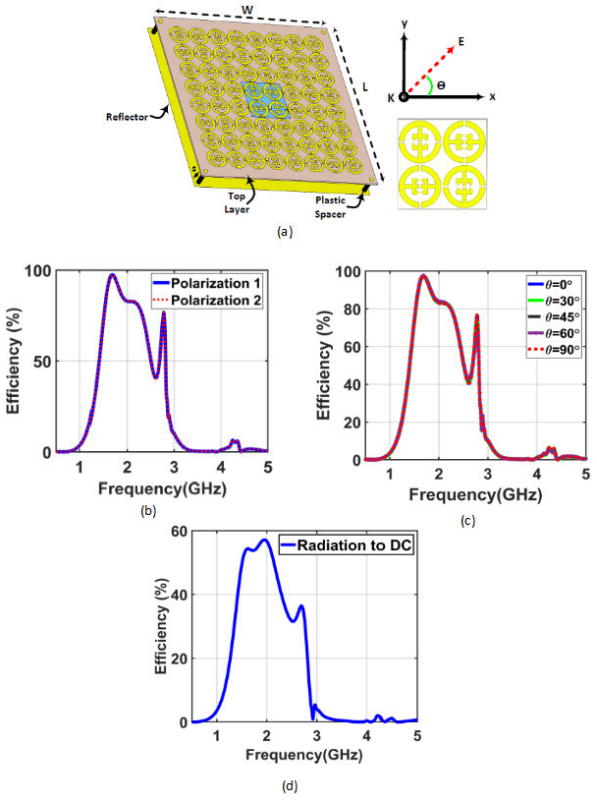

FIGURE 20. Dual-polarized planar rectifying metasurface (a) model of 8 × 8 element metasurface, where each 2 × 2 element block is a super-cell, (b) conversion efficiency with different polarizations, (c) conversion efficiency with different incidence angles, (d) EM-to-DC efficiency [122].

confirm that the SWIPT system performance is enhanced by the introduction of RISs. Similarly, [141] examines a scenario where a multi-antenna base-station transfers energy to multiple users in non-line-of-sight conditions, with the aid of multiple RISs. The aim is to maximize the minimum harvested power by all users through optimizing the transmit beamformer, and RIS phase shifts. Considering system complexities, a suboptimal scheme is proposed, which achieves 80% of the optimal performance, with minimal communication overhead.

VI. OPEN PROBLEMS AND FUTURE DIRECTIONS

From the current research elaborated upon in the previous sections, it is evident that metasurface microwave energy transmitters and harvesters are a feasible technology for enabling wireless powered network devices. Notwithstanding the significant progress made so far, there are a number of areas that would benefit from further investigations.

There has been relatively less research in the development of microwave energy transmitting metasurfaces, compared to metasurface microwave energy harvesters. Consequently, while proofs-of-concept have been developed, there is still a need to address practical usage scenarios. For instance, a practical usage scenario may require an energy transmitter to possess the capability for energy transfer to multiple devices, each with different polarization requirements. An overview of the state-of-the art, however, reveals that the higher transfer

efficiencies are obtained with single-polarization metasurfaces in reflecting mode and static beams. There is a need to have multi-focus, multi-polarization reflective metasurfaces with improved transfer efficiencies. Also, although, there has been some progress regarding dynamic beam focusing [77], low-power tracking and localizing of intended receivers in real-time, and with minimal overhead, still remains an open research area. Recent advances in electromagnetic reconfiguration and programming will be of great benefit in this area [142], [143]. Furthermore, there is a need for a standardization of metrics by which the performance of energy transmitting metasurfaces are characterized.

One of the core promises of metasurface harvesters is the ability to maximize the harvested microwave energy over a given footprint. While metasurfaces have been shown to provide greater energy conversion efficiencies than patch antenna arrays of similar footprints [89], the actual power densities at individual constituent meta-cell elements are low because they are electrically small. Consequently, while the energy conversion efficiency is an important characterization of the performance of the metasurface harvester, it is equally critical to optimize the actual AC voltage output available to the rectification stage. Rectifying diodes typically have a turn-ON threshold, and it is important to maximize the voltage available to them, which in turn would maximize the DC power delivered to the associated load [144]. Even though near-unity conversion efficiencies have been realized with metasurfaces, the EM-to-DC efficiencies of rectifying metasurfaces need to be further enhanced to surpass levels realized using rectennas, where performances exceeding 80% have been reported [145]–[148].

Typical ambient power levels available from wireless technologies are in the range of -120 dBm to -50 dBm [20]. These power levels are significantly lower than the levels currently required to obtain efficient EM-to-DC conversion. It is, therefore, necessary that lower sensitivities be achieved with metasurface harvesters, in order to facilitate efficient scavenging of ambient microwaves. Nonetheless, the current performance levels achieved suggest that present implementations can be used within proximity of existing microwave sources or dedicated power beacons, where diffuse or focused-beam radiations would be adequate. Enabling efficient power provision over a range of input power levels [123], is an important step towards realizing systems that can adapt to dynamic ambient conditions.

Wireless sensors typically have much lower power consumption requirements compared to other devices, which can be satisfied with the current state-of-the-art [13], [59]–[61], [121]. To this end, the miniaturization of metasurface harvesters, and their realization using alternative flexible materials, without compromising performance, would be of great benefit for device-level integration, including novel integration arrangements [149]. Furthermore, dynamic impedance match designs can be investigated to support maximal power transfer under different loading conditions.

The concept of smart radio environments in 6G wireless networks has given rise to a new class of metasurfaces, which serve as RISs. Although there have been various theoretical investigations revealing system gains arising from using these smart surfaces in networks to aid simultaneous information and energy transfer, system-level simulations, which account for actual EM propagation mechanisms, are generally lacking. There is a need for models, which connect the EM wave manipulations achieved by these smart surfaces to overall system objectives [1]. Also, efficient channel estimation schemes needed to enable real-time control of the radio environment would require active RIS implementations [150], where the needed power is scavenged from ambient sources. It is not presently well-know how much overhead is required for optimal estimation, and the power requirements for its implementation. Furthermore, it is expected that large-scale RIS-assisted wireless powered networks would require the deployment of a significant number of RISs. The development of schemes for efficiently coordinating these units to achieve system-level objectives still remains an open area of research.

VII. CONCLUSION

This paper has examined recent progress in the development of metasurfaces for microwave energy transmission and harvesting. Metasurfaces have been employed as reflectors to focus power from transmitting microwave antennas at intended spatial coordinates. Also, they have been shown to be viable replacements for microwave energy transmitting antennas, where they are expected to enhance the efficiency with which energy is coupled into the focused beam. Similarly, the demonstrated microwave energy harvesting potential of single meta-cell structures has motivated their use in 2D energy harvesting arrays, leading to an evolution of metasurface harvesters from single-frequency energy collectors to wideband and multiband structures, with polarization independence and wide-incident capture features. Rectifying metasurfaces, from which DC voltages can be directly sourced, have also been realized. Although photolithography and etching techniques are typically used to realize printed circuit board (PCB) metasurfaces implementations, additive manufacturing has been shown to hold promise for rapid prototyping of complex metasurface structures. Attempts have also been made to realize prototypes using flexible materials, which would enable the installation of these metasurfaces in a variety of environments. Metasurfaces have also been touted as viable implementations of RISs in 6G wireless networks, which have been shown to improve the performance of wireless powered networks when deployed in radio environments. The state-of-the art in this field can be further advanced with greater progress in miniaturization, higher efficiencies, lower sensitivity thresholds, conformal implementations, advances in system simulators, and algorithms for software control of the structures. Current research trends suggest an increasingly significant role for metasurfaces in actualizing microwave energy transmission and harvesting in

wireless powered networks, which would extend the potential functionalities provided by such networks.

REFERENCES

[1] M. D. Renzo, M. Debbah, D.-T. Phan-Huy, A. Zappone, M.-S. Alouini, C. Yuen, V. Sciancalepore, G. C. Alexandropoulos, J. Hoydis, H. Gacanin, J. D. Rosny, A. Bounceur, G. Lerosey, and M. Fink, "Smart radio environments empowered by reconfigurable AI meta-surfaces: An idea whose time has come," *EURASIP J. Wireless Commun. Netw.*, vol. 2019, no. 1, pp. 1–20, Dec. 2019.

[2] A. Gatherer, "What will 6G be?" in *Proc. IEEE ComSoc Technol. News*, 2018. [Online]. Available: https://www.comsoc.org/ctn/what-will-6g-be

[3] F. Tariq, M. Khandaker, K.-K. Wong, M. Imran, M. Bennis, and M. Debbah, "A speculative study on 6G," 2019, *arXiv:1902.06700*. [Online]. Available: http://arxiv.org/abs/1902.06700

[4] X. Wang, X. Li, and V. C. M. Leung, "Artificial intelligence-based techniques for emerging heterogeneous network: State of the arts, opportunities, and challenges," *IEEE Access*, vol. 3, pp. 1379–1391, 2015.

[5] S. Andreev, V. Petrov, M. Dohler, and H. Yanikomeroglu, "Future of ultra-dense networks beyond 5G: Harnessing heterogeneous moving cells," *IEEE Commun. Mag.*, vol. 57, no. 6, pp. 86–92, May 2019.

[6] L. Roselli, C. Mariotti, P. Mezzanotte, F. Alimenti, G. Orecchini, M. Virili, and N. B. Carvalho, "Review of the present technologies concurrently contributing to the implementation of the Internet of Things (IoT) paradigm: RFID, green electronics, WPT and energy harvesting," in *Proc. IEEE Topical Conf. Wireless Sensors Sensor Netw. (WiSNet)*, Jan. 2015, pp. 1–3.

[7] J. Hester and J. Sorber, "The future of sensing is batteryless, intermittent, and awesome," in *Proc. 15th ACM Conf. Embedded Netw. Sensor Syst.*, Nov. 2017, pp. 1–6.

[8] W. H. Ko, "Early history and challenges of implantable electronics," *ACM J. Emerg. Technol. Comput. Syst.*, vol. 8, no. 2, pp. 1–9, Jun. 2012.

[9] J. A. Paradiso and T. Starner, "Energy scavenging for mobile and wireless electronics," *IEEE Pervas. Comput.*, vol. 4, no. 1, pp. 18–27, Jan. 2005.

[10] M. Pinuela, P. D. Mitcheson, and S. Lucyszyn, "Ambient RF energy harvesting in urban and semi-urban environments," *IEEE Trans. Microw. Theory Techn.*, vol. 61, no. 7, pp. 2715–2726, Jul. 2013.

[11] N. Md. Din, C. K. Chakrabarty, A. Bin Ismail, K. K. A. Devi, and W.-Y. Chen, "Design of RF energy harvesting system for energizing low power devices," *Prog. Electromagn. Res.*, vol. 132, pp. 49–69, Jul. 2012.

[12] V. Talla, B. Kellogg, B. Ransford, S. Naderiparizi, J. R. Smith, and S. Gollakota, "Powering the next billion devices with Wi-Fi," *Commun. ACM*, vol. 60, no. 3, pp. 83–91, Feb. 2017.

[13] S. Kim, R. Vyas, J. Bito, K. Niotaki, A. Collado, A. Georgiadis, and M. M. Tentzeris, "Ambient RF energy-harvesting technologies for self-sustainable standalone wireless sensor platforms," *Proc. IEEE*, vol. 102, no. 11, pp. 1649–1666, Nov. 2014.

[14] X. Lu, P. Wang, D. Niyato, D. I. Kim, and Z. Han, "Wireless networks with RF energy harvesting: A contemporary survey," *IEEE Commun. Surveys Tuts.*, vol. 17, no. 2, pp. 757–789, 2nd Quart., 2015.

[15] B. Strassner and K. Chang, "Microwave power transmission: Historical milestones and system components," *Proc. IEEE*, vol. 101, no. 6, pp. 1379–1396, Jun. 2013.

[16] K. Wu, D. Choudhury, and H. Matsumoto, "Wireless power transmission, technology, and applications [Scanning the Issue]," *Proc. IEEE*, vol. 101, no. 6, pp. 1271–1275, Jun. 2013.

[17] W. C. Brown, "The history of wireless power transmission," *Sol. Energy*, vol. 56, no. 1, pp. 3–21, Jan. 1996.

[18] W. C. Brown, "The history of power transmission by radio waves," *IEEE Trans. Microw. Theory Techn.*, vol. 32, no. 9, pp. 1230–1242, Sep. 1984.

[19] W. Brown, "The microwave powered helicopter," *J. Microw. Power Electromagn. Energy*, vol. 1, pp. 1–21, Jan. 1966.

[20] K. Huang and X. Zhou, "Cutting the last wires for mobile communications by microwave power transfer," *IEEE Commun. Mag.*, vol. 53, no. 6, pp. 86–93, Jun. 2015.

[21] K. Huang and V. K. N. Lau, "Enabling wireless power transfer in cellular networks: Architecture, modeling and deployment," *IEEE Trans. Wireless Commun.*, vol. 13, no. 2, pp. 902–912, Feb. 2014.

[22] K. W. Choi, A. A. Aziz, D. Setiawan, N. M. Tran, L. Ginting, and D. I. Kim, "Distributed wireless power transfer system for Internet of Things devices," *IEEE Internet Things J.*, vol. 5, no. 4, pp. 2657–2671, Jan. 2018.

[23] S. Bi, Y. Zeng, and R. Zhang, "Wireless powered communication networks: An overview," *IEEE Wireless Commun.*, vol. 23, no. 2, pp. 10–18, Apr. 2016.

[24] S. Bi, C. K. Ho, and R. Zhang, "Wireless powered communication: Opportunities and challenges," *IEEE Commun. Mag.*, vol. 53, no. 4, pp. 117–125, Apr. 2015.

[25] D. R. Smith, V. R. Gowda, O. Yurduseven, S. Larouche, G. Lipworth, Y. Urzhumov, and M. S. Reynolds, "An analysis of beamed wireless power transfer in the fresnel zone using a dynamic, metasurface aperture," *J. Appl. Phys.*, vol. 121, no. 1, Jan. 2017, Art. no. 014901.

[26] C. Caloz and T. Itoh, *Electromagnetic Metamaterials: Transmission Line Theory and Microwave Applications*. Hoboken, NJ, USA: Wiley, 2005.

[27] I. B. Vendik and O. G. Vendik, "Metamaterials and their application in microwaves: A review," *Tech. Phys.*, vol. 58, no. 1, pp. 1–24, Jan. 2013.

[28] R. W. Ziolkowski and N. Engheta, "Metamaterials: Two decades past and into their electromagnetics future and beyond," *IEEE Trans. Antennas Propag.*, vol. 68, no. 3, pp. 1232–1237, Mar. 2020.

[29] Z. Wang, F. Cheng, T. Winsor, and Y. Liu, "Optical chiral metamaterials: A review of the fundamentals, fabrication methods and applications," *Nanotechnology*, vol. 27, no. 41, Oct. 2016, Art. no. 412001.

[30] A. Li, S. Singh, and D. Sievenpiper, "Metasurfaces and their applications," *Nanophotonics*, vol. 7, no. 6, pp. 989–1011, 2018.

[31] C. L. Holloway, E. F. Kuester, J. A. Gordon, J. O'Hara, J. Booth, and D. R. Smith, "An overview of the theory and applications of metasurfaces: The two-dimensional equivalents of metamaterials," *IEEE Antennas Propag. Mag.*, vol. 54, no. 2, pp. 10–35, Apr. 2012.

[32] G. C. Alexandropoulos, G. Lerosey, M. Debbah, and M. Fink, "Reconfigurable intelligent surfaces and metamaterials: The potential of wave propagation control for 6G wireless communications," 2020, *arXiv:2006.11136*. [Online]. Available: https://arxiv.org/abs/2006.11136

[33] L. Li, X. Zhang, C. Song, and Y. Huang, "Progress, challenges, and perspective on metasurfaces for ambient radio frequency energy harvesting," *Appl. Phys. Lett.*, vol. 116, no. 6, Feb. 2020, Art. no. 060501.

[34] A. A. G. Amer, S. Z. Sapuan, N. Nasimuddin, A. Alphones, and N. B. Zinal, "A comprehensive review of metasurface structures suitable for RF energy harvesting," *IEEE Access*, vol. 8, pp. 76433–76452, 2020.

[35] Z. Chen, B. Guo, Y. Yang, and C. Cheng, "Metamaterials-based enhanced energy harvesting: A review," *Phys. B, Condens. Matter*, vol. 438, pp. 1–8, Apr. 2014.

[36] V. G. Veselago, "The electrodynamics of substances with simultaneously negative values of ϵ and μ," *Sov. Phys. Uspekhi*, vol. 10, no. 4, pp. 509–514, Apr. 1968.

[37] J. B. Pendry, "Controlling electromagnetic fields," *Science*, vol. 312, no. 5781, pp. 1780–1782, Jun. 2006.

[38] G. Yoon, I. Kim, and J. Rho, "Challenges in fabrication towards realization of practical metamaterials," *Microelectronic Eng.*, vol. 163, pp. 7–20, Sep. 2016.

[39] A. M. Patel and A. Grbic, "Transformation electromagnetics devices using tensor impedance surfaces," in *IEEE MTT-S Int. Microw. Symp. Dig.*, Jun. 2013, pp. 1–9.

[40] C. Pfeiffer and A. Grbic, "Millimeter-wave transmitarrays for wavefront and polarization control," *IEEE Trans. Microw. Theory Techn.*, vol. 61, no. 12, pp. 4407–4417, Dec. 2013.

[41] M. Faenzi, F. Caminita, E. Martini, P. De Vita, G. Minatti, M. Sabbadini, and S. Maci, "Realization and measurement of broadside beam modulated metasurface antennas," *IEEE Antennas Wireless Propag. Lett.*, vol. 15, pp. 610–613, 2016.

[42] G. Minatti, M. Faenzi, E. Martini, F. Caminita, P. De Vita, D. Gonzalez-Ovejero, M. Sabbadini, and S. Maci, "Modulated metasurface antennas for space: Synthesis, analysis and realizations," *IEEE Trans. Antennas Propag.*, vol. 63, no. 4, pp. 1288–1300, Apr. 2015.

[43] K. Achouri, B. A. Khan, S. Gupta, G. Lavigne, M. A. Salem, and C. Caloz, "Synthesis of electromagnetic metasurfaces: Principles and illustrations," *EPJ Appl. Metamater.*, vol. 2, no. 12, pp. 1–11, Jan. 2015.

[44] O. Avayu, E. Almeida, Y. Prior, and T. Ellenbogen, "Composite functional metasurfaces for multispectral achromatic optics," *Nature Commun.*, vol. 8, no. 1, pp. 1–7, Apr. 2017.

[45] Z. Sun, J. Zhao, B. Zhu, T. Jiang, and Y. Feng, "Selective wave-transmitting electromagnetic absorber through composite metasurface," *AIP Adv.*, vol. 7, no. 11, Nov. 2017, Art. no. 115017.

[46] A. Krasnok, S. Makarov, M. Petrov, R. Savelev, P. Belov, and Y. Kivshar, "Towards all-dielectric metamaterials and nanophotonics," *Proc. SPIE*, vol. 9502, May 2015, Art. no. 950203.

[47] A. Andryieuski, S. M. Kuznetsova, S. V. Zhukovsky, Y. S. Kivshar, and A. V. Lavrinenko, "Water: Promising opportunities for tunable all-dielectric electromagnetic metamaterials," *Sci. Rep.*, vol. 5, no. 1, pp. 1–9, 2015.

[48] I. V. Stenishchev and A. A. Basharin, "Toroidal response in all-dielectric metamaterials based on water," *Sci. Rep.*, vol. 7, no. 1, pp. 1–9, Dec. 2017.

[49] G. Zhang, C. Lan, H. Bian, R. Gao, and J. Zhou, "Flexible, all-dielectric metasurface fabricated via nanosphere lithography and its applications in sensing," *Opt. Exp.*, vol. 25, no. 18, pp. 22038–22045, 2017.

[50] F. Elek, B. B. Tierney, and A. Grbic, "Synthesis of tensor impedance surfaces to control phase and power flow of guided waves," *IEEE Trans. Antennas Propag.*, vol. 63, no. 9, pp. 3956–3962, Sep. 2015.

[51] A. M. Patel and A. Grbic, "Modeling and analysis of printed-circuit tensor impedance surfaces," *IEEE Trans. Antennas Propag.*, vol. 61, no. 1, pp. 211–220, Jan. 2013.

[52] E. F. Kuester, M. A. Mohamed, M. Piket-May, and C. L. Holloway, "Averaged transition conditions for electromagnetic fields at a metafilm," *IEEE Trans. Antennas Propag.*, vol. 51, no. 10, pp. 2641–2651, Oct. 2003.

[53] S. Tretyakov, *Analytical Modeling in Applied Electromagnetics*. Boston, MA, USA: Artech House, 2003.

[54] K. Achouri, M. A. Salem, and C. Caloz, "General metasurface synthesis based on susceptibility tensors," *IEEE Trans. Antennas Propag.*, vol. 63, no. 7, pp. 2977–2991, Jul. 2015.

[55] Y. Vahabzadeh, N. Chamanara, K. Achouri, and C. Caloz, "Computational analysis of metasurfaces," *IEEE J. Multiscale Multiphys. Comput. Techn.*, vol. 3, pp. 37–49, 2018.

[56] T. Niemi, A. O. Karilainen, and S. A. Tretyakov, "Synthesis of polarization transformers," *IEEE Trans. Antennas Propag.*, vol. 61, no. 6, pp. 3102–3111, Jun. 2013.

[57] K. Huang, C. Zhong, and G. Zhu, "Some new research trends in wirelessly powered communications," *IEEE Wireless Commun.*, vol. 23, no. 2, pp. 19–27, Apr. 2016.

[58] A. Ghazanfari, H. Tabassum, and E. Hossain, "Ambient RF energy harvesting in ultra-dense small cell networks: Performance and trade-offs," *IEEE Wireless Commun.*, vol. 23, no. 2, pp. 38–45, Apr. 2016.

[59] K. W. Choi, P. A. Rosyady, L. Ginting, A. A. Aziz, D. Setiawan, and D. I. Kim, "Theory and experiment for wireless-powered sensor networks: How to keep sensors alive," *IEEE Trans. Wireless Commun.*, vol. 17, no. 1, pp. 430–444, Jan. 2018.

[60] K. W. Choi, L. Ginting, P. A. Rosyady, A. A. Aziz, and D. I. Kim, "Wireless-powered sensor networks: How to realize," *IEEE Trans. Wireless Commun.*, vol. 16, no. 1, pp. 221–234, Jan. 2017.

[61] K. W. Choi, L. Ginting, A. A. Aziz, D. Setiawan, J. H. Park, S. I. Hwang, D. S. Kang, M. Y. Chung, and D. I. Kim, "Toward realization of long-range wireless-powered sensor networks," *IEEE Wireless Commun.*, vol. 26, no. 4, pp. 184–192, Aug. 2019.

[62] V. R. Gowda, O. Yurduseven, G. Lipworth, T. Zupan, M. S. Reynolds, and D. R. Smith, "Wireless power transfer in the radiative near field," *IEEE Antennas Wireless Propag. Lett.*, vol. 15, pp. 1865–1868, 2016.

[63] R. Gonzalez Ayestaran, G. Leon, M. R. Pino, and P. Nepa, "Wireless power transfer through simultaneous near-field focusing and far-field synthesis," *IEEE Trans. Antennas Propag.*, vol. 67, no. 8, pp. 5623–5633, Aug. 2019.

[64] X. Yang, W. Geyi, and H. Sun, "Optimum design of wireless power transmission system using microstrip patch antenna arrays," *IEEE Antennas Wireless Propag. Lett.*, vol. 16, pp. 1824–1827, 2017.

[65] Y. Li and V. Jandhyala, "Design of retrodirective antenna arrays for short-range wireless power transmission," *IEEE Trans. Antennas Propag.*, vol. 60, no. 1, pp. 206–211, Jan. 2012.

[66] A. Arbabi, R. M. Briggs, Y. Horie, M. Bagheri, and A. Faraon, "Efficient dielectric metasurface collimating lenses for mid-infrared quantum cascade lasers," *Opt. Exp.*, vol. 23, no. 26, p. 33310, 2015.

[67] M. Khorasaninejad, W. T. Chen, R. C. Devlin, J. Oh, A. Y. Zhu, and F. Capasso, "Metalenses at visible wavelengths: Diffraction-limited focusing and subwavelength resolution imaging," *Science*, vol. 352, no. 6290, pp. 1190–1194, Jun. 2016.

[68] Y. C. Cheng, S. Kicas, J. Trull, M. Peckus, C. Cojocaru, R. Vilaseca, R. Drazdys, and K. Staliunas, "Flat focusing mirror," *Sci. Rep.*, vol. 4, no. 1, pp. 1–4, May 2015.

[69] S. Yu, L. Li, G. Shi, C. Zhu, X. Zhou, and Y. Shi, "Design, fabrication, and measurement of reflective metasurface for orbital angular momentum vortex wave in radio frequency domain," *Appl. Phys. Lett.*, vol. 108, no. 12, pp. 1–6, 2016.

[70] S. Yu, H. Liu, and L. Li, "Design of near-field focused metasurface for high-efficient wireless power transfer with multifocus characteristics," *IEEE Trans. Ind. Electron.*, vol. 66, no. 5, pp. 3993–4002, May 2019.

[71] P. Zhang, L. Li, X. Zhang, H. Liu, and Y. Shi, "Design, measurement and analysis of near-field focusing reflective metasurface for dual-polarization and multi-focus wireless power transfer," *IEEE Access*, vol. 7, pp. 110387–110399, 2019.

[72] O. Yurduseven, S. Ye, T. Fromenteze, B. J. Wiley, and D. R. Smith, "3D conductive polymer printed metasurface antenna for fresnel focusing," *Designs*, vol. 3, no. 3, p. 46, Sep. 2019.

[73] O. Yurduseven, D. L. Marks, J. N. Gollub, D. R. Smith, "Design and analysis of a reconfigurable holographic metasurface aperture for dynamic focusing in the Fresnel zone," *IEEE Access*, vol. 5, pp. 15055–15065, 2017.

[74] O. Yurduseven, D. R. Smith, and T. Fromenteze, "Design of a reconfigurable metasurface antenna for dynamic near-field focusing," in *Proc. IEEE Int. Symp. Antennas Propag. USNC/URSI Nat. Radio Sci. Meeting*, Jul. 2018, pp. 1707–1708.

[75] W. Luo and L. Xu, "Wireless power transfer in the radiative near-field using a reconfigurable holographic metasurface aperture," in *Proc. IEEE Int. Conf. Commun. (ICC)*, May 2018, pp. 1–5.

[76] W. Luo, "Wireless power transfer in the radiative near-field using a novel reconfigurable holographic metasurface aperture," *IEICE Trans. Fundam. Electron. Commun. Comput. Sci.*, vol. E102.A, no. 12, pp. 1928–1931, Dec. 2019.

[77] N. M. Tran, M. M. Amri, J. H. Park, S. I. Hwang, D. I. Kim, and K. W. Choi, "A novel coding metasurface for wireless power transfer applications," *Energies*, vol. 12, no. 23, p. 4488, Nov. 2019.

[78] G. S. Lipworth, J. A. Hagerty, D. Arnitz, Y. A. Urzhumov, D. R. Nash, R. J. Hannigan, C. T. Tegreene, and M. S. Reynolds, "A large planar holographic reflectarray for fresnel-zone microwave wireless power transfer at 5.8 GHz," in *IEEE MTT-S Int. Microw. Symp. Dig.*, Jun. 2018, pp. 964–967.

[79] A. A. Aziz, L. Ginting, D. Setiawan, J. H. Park, N. M. Tran, G. Y. Yeon, D. I. Kim, and K. W. Choi, "Battery-less location tracking for Internet of Things: Simultaneous wireless power transfer and positioning," *IEEE Internet Things J.*, vol. 6, no. 5, pp. 9147–9164, Oct. 2019.

[80] O. M. Ramahi, T. S. Almoneef, M. AlShareef, and M. S. Boybay, "Metamaterial particles for electromagnetic energy harvesting," *Appl. Phys. Lett.*, vol. 101, no. 17, Oct. 2012, Art. no. 173903.

[81] B. M. Z. Abidin, O. O. Khalifa, E. M. A. Elsheikh, and A. H. Abdulla, "Wireless energy harvesting for portable devices using split ring resonator," in *Proc. Int. Conf. Comput., Control, Netw., Electron. Embedded Syst. Eng. (ICCNEEE)*, Sep. 2015, pp. 362–367.

[82] N. Zhu, R. W. Ziolkowski, and H. Xin, "A metamaterial-inspired, electrically small rectenna for high-efficiency, low power harvesting and scavenging at the global positioning system L1 frequency," *Appl. Phys. Lett.*, vol. 114101, pp. 3–5, Sep. 2011.

[83] B. Alavikia, T. S. Almoneef, and O. M. Ramahi, "Electromagnetic energy harvesting using complementary split-ring resonators," *Appl. Phys. Lett.*, vol. 104, no. 16, Apr. 2014, Art. no. 163903.

[84] T. Almoneef and O. M. Ramahi, "A 3-dimensional stacked metamaterial arrays for electromagnetic energy harvesting," *Prog. Electromagn. Res.*, vol. 146, pp. 109–115, Mar. 2014.

[85] N. I. Landy, S. Sajuyigbe, J. J. Mock, D. R. Smith, and W. J. Padilla, "Perfect metamaterial absorber," *Phys. Rev. Lett.*, vol. 100, no. 20, 2008, Art. no. 207402.

[86] Q.-Y. Wen *et al.*, "Perfect metamaterial absorbers in microwave and terahertz bands," in *Metamaterial*, X.-Y. Jiang, Ed. London, U.K.: InTech, 2012, pp. 501–512.

[87] T. S. Almoneef and O. M. Ramahi, "Metamaterial electromagnetic energy harvester with near unity efficiency," *Appl. Phys. Lett.*, vol. 106, no. 15, Apr. 2015, Art. no. 153902.

[88] M. E. Badawe and O. M. Ramahi, "Metasurface for near-unity electromagnetic energy harvesting and wireless power transfer," in *Proc. IEEE Int. Symp. Antennas Propag. (APSURSI)*, Jun. 2016, pp. 609–610.

[89] B. Alavikia, T. S. Almoneef, and O. M. Ramahi, "Complementary split ring resonator arrays for electromagnetic energy harvesting," *Appl. Phys. Lett.*, vol. 107, no. 3, pp. 1–6, 2015.

[90] W. Hu, D. Inserra, Y. Huang, J. Li, G. Wen, J. Xie, and W. Zhu, "High efficiency electromagnetic energy harvesting with metasurface," in *Proc. IEEE Asia–Pacific Conf. Antennas Propag. (APCAP)*, Aug. 2018, pp. 488–489.

[91] W. Hu, Z. Yang, F. Zhao, G. Wen, J. Li, Y. Huang, D. Inserra, and Z. Chen, "Low-cost air gap metasurface structure for high absorption efficiency energy harvesting," *Int. J. Antennas Propag.*, vol. 2019, pp. 1–8, Sep. 2019.
[92] B. Alavikia, T. S. Almoneef, and O. M. Ramahi, "Wideband resonator arrays for electromagnetic energy harvesting and wireless power transfer," *Appl. Phys. Lett.*, vol. 107, no. 24, Dec. 2015, Art. no. 243902.
[93] E. Karakaya, F. Bagci, A. E. Yilmaz, and B. Akaoglu, "Metamaterial-based four-band electromagnetic energy harvesting at commonly used GSM and Wi-Fi frequencies," *J. Electron. Mater.*, vol. 48, no. 4, pp. 2307–2316, Apr. 2019.
[94] E. Karakaya, F. Bagci, S. Can, A. E. Yilmaz, and B. Akaoglu, "Four-band electromagnetic energy harvesting with a dual-layer metamaterial structure," *Int. J. RF Microw. Comput. Eng.*, vol. 29, no. 1, pp. 1–7, 2019.
[95] B. Ghaderi, V. Nayyeri, M. Soleimani, and O. M. Ramahi, "Multi-polarisation electromagnetic energy harvesting with high efficiency," *IET Microw., Antennas Propag.*, vol. 12, no. 15, pp. 2271–2275, Dec. 2018.
[96] X. Zhang, H. Liu, and L. Li, "Tri-band miniaturized wide-angle and polarization-insensitive metasurface for ambient energy harvesting," *Appl. Phys. Lett.*, vol. 111, no. 7, Aug. 2017, Art. no. 071902.
[97] H.-T. Zhong, X.-X. Yang, C. Tan, and K. Yu, "Triple-band polarization-insensitive and wide-angle metamaterial array for electromagnetic energy harvesting," *Appl. Phys. Lett.*, vol. 109, no. 25, Dec. 2016, Art. no. 253904.
[98] S. D. Assimonis, T. Kollatou, D. Tsiamitros, D. Stimoniaris, T. Samaras, and J. N. Sahalos, "High efficiency and triple-band metamaterial electromagnetic energy hervester," in *Proc. 9th Int. Conf. Electr. Electron. Eng. (ELECO)*, Nov. 2015, pp. 320–323.
[99] B. Ghaderi, V. Nayyeri, M. Soleimani, and O. M. Ramahi, "Pixelated metasurface for dual-band and multi-polarization electromagnetic energy harvesting," *Sci. Rep.*, vol. 8, no. 1, pp. 1–12, Dec. 2018.
[100] H.-T. Zhong, X.-X. Yang, X.-T. Song, Z.-Y. Guo, and F. Yu, "Wide-band metamaterial array with polarization-independent and wide incident angle for harvesting ambient electromagnetic energy and wireless power transfer," *Appl. Phys. Lett.*, vol. 111, no. 21, Nov. 2017, Art. no. 213902.
[101] F. Yu, X. Yang, H. Zhong, C. Chu, and S. Gao, "Polarization-insensitive wide-angle-reception metasurface with simplified structure for harvesting electromagnetic energy," *Appl. Phys. Lett.*, vol. 113, no. 12, pp. 1–5, 2018.
[102] X. Zhang, H. Liu, and L. Li, "Electromagnetic power harvester using wide-angle and polarization-insensitive metasurfaces," *Appl. Sci.*, vol. 8, no. 4, p. 497, Mar. 2018.
[103] S. Costanzo and F. Venneri, "Innovative fractal-based metasurface for energy harvesting," in *Proc. URSI GASS*, Sep. 2020, pp. 1–3.
[104] B. Ghaderi, V. Nayyeri, M. Soleimani, and O. M. Ramahi, "A novel symmetric ELC resonator for polarization-independent and highly efficient electromagnetic energy harvesting," in *IEEE MTT-S Int. Microw. Symp. Dig.*, Sep. 2017, pp. 1–3.
[105] X. Zhang and L. Li, "A dual-band polarization-independent and wide-angle metasurface for electromagnetic power harvesting," in *Proc. 6th Asia–Pacific Conf. Antennas Propag. (APCAP)*, Oct. 2017, pp. 1–3.
[106] F. Yu, G. Q. He, X. X. Yang, J. Du, and S. Gao, "Polarization-insensitive metasurface for harvesting electromagnetic energy with high efficiency and frequency stability over wide range of incidence angles," *Appl. Sci.*, vol. 10, no. 22, pp. 1–10, 2020.
[107] X. Duan, X. Chen, Y. Zhou, L. Zhou, and S. Hao, "Wideband metamaterial electromagnetic energy harvester with high capture efficiency and wide incident angle," *IEEE Antennas Wireless Propag. Lett.*, vol. 17, no. 9, pp. 1617–1621, Sep. 2018.
[108] A. Ghaneizadeh, K. Mafinezhad, and M. Joodaki, "Design and fabrication of a 2D-isotropic flexible ultra-thin metasurface for ambient electromagnetic energy harvesting," *AIP Adv.*, vol. 9, no. 2, Feb. 2019, Art. no. 025304.
[109] A. Ghaneizadeh, K. Mafinezhad, and M. Joodaki, "A new compact dual-band perfect absorption ultrathin planar metasurface energy harvester in X- and V-bands with a wide incident angle," *AIP Adv.*, vol. 10, no. 8, Aug. 2020, Art. no. 085007.
[110] B. Li, X. Shao, N. Shahshahan, N. Goldsman, T. Salter, and G. M. Metze, "An antenna co-design dual band RF energy harvester," *IEEE Trans. Circuits Syst. I, Reg. Papers*, vol. 60, no. 12, pp. 3256–3266, Dec. 2013.
[111] A. Boaventura, A. Collado, N. B. Carvalho, and A. Georgiadis, "Optimum behavior: Wireless power transmission system design through behavioral models and efficient synthesis techniques," *IEEE Microw. Mag.*, vol. 14, no. 2, pp. 26–35, Mar. 2013.
[112] A. M. Hawkes, A. R. Katko, and S. A. Cummer, "A microwave metamaterial with integrated power harvesting functionality," *Appl. Phys. Lett.*, vol. 103, no. 16, Oct. 2013, Art. no. 163901.
[113] Q. Zhao, L. Li, X. Zhang, X. Zhang, and J. Chen, "An ambient energy harvester using metasurface," in *Proc. IEEE Int. Symp. Electromagn. Compat. IEEE Asia–Pacific Symp. Electromagn. Compat. (EMC/APEMC)*, May 2018, pp. 111–112.
[114] M. El Badawe, T. S. Almoneef, and O. M. Ramahi, "A metasurface for conversion of electromagnetic radiation to DC," *AIP Adv.*, vol. 7, no. 3, Mar. 2017, Art. no. 035112.
[115] M. El Badawe and O. M. Ramahi, "Efficient metasurface rectenna for electromagnetic wireless power transfer and energy harvesting," *Prog. Electromagn. Res.*, vol. 161, pp. 35–40, Mar. 2018.
[116] L. KangHyeok and S. K. Hong, "Rectifying metasurface with high efficiency at low power for 2.45 GHz band," *IEEE Antennas Wireless Propag. Lett.*, vol. 19, no. 12, pp. 2216–2220, Dec. 2020.
[117] X. Duan, X. Chen, and L. Zhou, "A metamaterial harvester with integrated rectifying functionality," in *Proc. IEEE/ACES Int. Conf. Wireless Inf. Technol. Syst. (ICWITS) Appl. Comput. Electromagn. (ACES)*, Mar. 2016, pp. 1–2.
[118] X. Duan, X. Chen, and L. Zhou, "A metamaterial electromagnetic energy rectifying surface with high harvesting efficiency," *AIP Adv.*, vol. 6, no. 12, Dec. 2016, Art. no. 125020.
[119] T. S. Almoneef, F. Erkmen, and O. M. Ramahi, "Harvesting the energy of multi-polarized electromagnetic waves," *Sci. Rep.*, vol. 7, no. 1, pp. 1–14, Dec. 2017.
[120] P. Xu, S.-Y. Wang, and W. Geyi, "Design of an effective energy receiving adapter for microwave wireless power transmission application," *AIP Adv.*, vol. 6, no. 10, Oct. 2016, Art. no. 105010.
[121] G. T. Oumbé Tékam, V. Ginis, J. Danckaert, and P. Tassin, "Designing an efficient rectifying cut-wire metasurface for electromagnetic energy harvesting," *Appl. Phys. Lett.*, vol. 110, no. 8, pp. 1–5, Feb. 2017.
[122] M. A. Aldhaeebi and T. S. Almoneef, "Planar dual polarized metasurface array for microwave energy harvesting," *Electronics*, vol. 9, no. 12, pp. 1–13, 2020.
[123] L. Li, X. Zhang, C. Song, W. Zhang, T. Jia, and Y. Huang, "Compact dual-band, wide-angle, polarization-angle-independent rectifying metasurface for ambient energy harvesting and wireless power transfer," *IEEE Trans. Microw. Theory Techn.*, early access, Dec. 8, 2020, doi: 10.1109/TMTT.2020.3040962.
[124] M. Di Renzo *et al.*, "Smart radio environments empowered by reconfigurable intelligent surfaces: How it works, state of research, and the road ahead," *IEEE J. Sel. Areas Commun.*, vol. 38, no. 11, pp. 2450–2525, Nov. 2020.
[125] H. Gacanin and M. Di Renzo, "Wireless 2.0: Towards an intelligent radio environment empowered by reconfigurable meta-surfaces and artificial intelligence," 2020, *arXiv:2002.11040*. [Online]. Available: https://arxiv.org/abs/2002.11040
[126] A. Zappone, M. Di Renzo, F. Shams, X. Qian, and M. Debbah, "Overhead-aware design of reconfigurable intelligent surfaces in smart radio environments," *IEEE Trans. Wireless Commun.*, vol. 20, no. 1, pp. 126–141, Jan. 2021.
[127] S. Gong *et al.*, "Toward smart wireless communications via intelligent reflecting surfaces: A contemporary survey," *IEEE Commun. Surveys Tuts.*, vol. 22, no. 4, pp. 2283–2314, 2020.
[128] A. Welkie, L. Shangguan, J. Gummeson, W. Hu, and K. Jamieson, "Programmable radio environments for smart spaces," in *Proc. 16th ACM Workshop Hot Topics Netw.*, Nov. 2017, pp. 36–42.
[129] The VISORSURF project. (2017). A hardware platform for software-driven functional metasurfaces. Horizon 2020 Future Emerging Technologies. Accessed: Jan. 4, 2021. [Online]. Available: http://visorsurf.eu
[130] The Ariadne project. (2019). *Artificial Intelligence Aided D-Band Network for 5G Long Term Evolution Technical Overview*. Accessed: Jan. 4, 2021. [Online]. Available: https://www.ict-ariadne.eu/
[131] C. Huang, A. Zappone, G. C. Alexandropoulos, M. Debbah, and C. Yuen, "Reconfigurable intelligent surfaces for energy efficiency in wireless communication," *IEEE Trans. Wireless Commun.*, vol. 18, no. 8, pp. 4157–4170, Aug. 2019.
[132] Y. Tang, G. Ma, H. Xie, J. Xu, and X. Han, "Joint transmit and reflective beamforming design for IRS-assisted multiuser MISO SWIPT systems," in *Proc. IEEE Int. Conf. Commun. (ICC)*, Jun. 2020, pp. 1–6.
[133] Q. Wu and R. Zhang, "Joint active and passive beamforming optimization for intelligent reflecting surface assisted SWIPT under QoS constraints," *IEEE J. Sel. Areas Commun.*, vol. 38, no. 8, pp. 1735–1748, Aug. 2020.

[134] H. Yang, X. Yuan, J. Fang, and Y.-C. Liang, "Reconfigurable intelligent surface aided constant-envelope wireless power transfer," in *Proc. IEEE Global Commun. Conf. (GLOBECOM)*, Dec. 2020, pp. 1–15.
[135] W. Shi, X. Zhou, L. Jia, Y. Wu, F. Shu, and J. Wang, "Enhanced secure wireless information and power transfer via intelligent reflecting surface," *IEEE Commun. Lett.*, early access, Dec. 9, 2020, doi: 10.1109/LCOMM.2020.3043475.
[136] N. Hehao and L. Ni, "Intelligent reflect surface aided secure transmission in MIMO channel with SWIPT," *IEEE Access*, vol. 8, pp. 192132–192140, 2020.
[137] Q. Wu and R. Zhang, "Weighted sum power maximization for intelligent reflecting surface aided SWIPT," *IEEE Wireless Commun. Lett.*, vol. 9, no. 5, pp. 586–590, May 2020.
[138] Y. Zhao, B. Clerckx, and Z. Feng, "Intelligent reflecting surface-aided SWIPT: Joint waveform, active and passive beamforming design," 2020, *arXiv:2012.05646*. [Online]. Available: https://arxiv.org/abs/2012.05646
[139] Y. Zheng, S. Bi, Y. J. Zhang, Z. Quan, and H. Wang, "Intelligent reflecting surface enhanced user cooperation in wireless powered communication networks," *IEEE Wireless Commun. Lett.*, vol. 9, no. 6, pp. 901–905, Jun. 2020.
[140] C. Pan, H. Ren, K. Wang, M. Elkashlan, A. Nallanathan, J. Wang, and L. Hanzo, "Intelligent reflecting surface aided MIMO broadcasting for simultaneous wireless information and power transfer," 2019, *arXiv:1908.04863*. [Online]. Available: http://arxiv.org/abs/1908.04863
[141] L. Zhao, Z. Wang, and X. Wang, "Wireless power transfer empowered by reconfigurable intelligent surfaces," *IEEE Syst. J.*, early access, Apr. 28, 2020, doi: 10.1109/JSYST.2020.2985121.
[142] L. T. Gan, L. H. Blumenschein, Z. Huang, A. M. Okamura, E. W. Hawkes, and A. Fan, "3D electromagnetic reconfiguration enabled by soft continuum robots," *IEEE Robot. Automat. Lett.*, vol. 5, no. 2, pp. 1704–1711, Apr. 2020.
[143] A. Rafsanjani, K. Bertoldi, and A. R. Studart, "Programming soft robots with flexible mechanical metamaterials," *Sci. Robot.*, vol. 4, no. 29, Apr. 2019, Art. no. eaav7874.
[144] A. Z. Ashoor, T. S. Almoneef, and O. M. Ramahi, "A planar dipole array surface for electromagnetic energy harvesting and wireless power transfer," *IEEE Trans. Microw. Theory Techn.*, vol. 66, no. 3, pp. 1553–1560, Mar. 2018.
[145] C. R. Valenta and G. D. Durgin, "Harvesting wireless power: Survey of energy-harvester conversion efficiency in far-field, wireless power transfer systems," *IEEE Microw. Mag.*, vol. 15, no. 4, pp. 108–120, Jun. 2014.
[146] J. O. McSpadden, L. Fan, and K. Chang, "Design and experiments of a high-conversion-efficiency 5.8-GHz rectenna," *IEEE Trans. Microw. Theory Techn.*, vol. 46, no. 12, pp. 2053–2060, 1998.
[147] S. S. Bharj, R. Camisa, S. Grober, F. Wozniak, and E. Pendleton, "High efficiency C-band 1000 element rectenna array for microwave powered applications," in *Proc. IEEE Antennas Propag. Soc. AP-S Int. Symp.*, Jun. 1992, pp. 123–125.
[148] Y.-H. Suh and K. Chang, "A high-efficiency dual-frequency rectenna for 2.45- and 5.8-GHz wireless power transmission," *IEEE Trans. Microw. Theory Techn.*, vol. 50, no. 7, pp. 1784–1789, Jul. 2002.
[149] T. A. Tsiftsis, C. Valagiannopoulos, H. Liu, and N. I. Miridakis, "Metasurface-coated devices: A new paradigm for energy-efficient and secure communications in 5G and beyond," 2020, *arXiv:2006.12044*. [Online]. Available: https://arxiv.org/abs/2006.12044
[150] E. Björnson, Ö. Özdogan, and E. G. Larsson, "Reconfigurable intelligent surfaces: Three myths and two critical questions," 2020, *arXiv:2006.03377*. [Online]. Available: https://arxiv.org/abs/2006.03377

AKAA AGBAEZE ETENG (Member, IEEE) received the B.Eng. degree in electrical/electronic engineering from the Federal University of Technology Owerri, Nigeria, in 2002, the M.Eng. degree in telecommunications and electronics from the University of Port Harcourt, Nigeria, in 2008, and the Ph.D. degree in electrical engineering from Universiti Teknologi Malaysia, in 2016. He is currently a Lecturer with the Department of Electrical/Electronic Engineering, University of Port Harcourt. His research interests include wireless energy transfer, radio frequency energy harvesting, and wireless powered communications.

HUI HWANG GOH (Senior Member, IEEE) received the B.Eng. (Hons.) and M.Eng. degrees in electrical engineering and the Ph.D. degree in electrical engineering from Universiti Teknologi Malaysia, Johor Bahru, Malaysia, in 1998, 2002, and 2007, respectively. He is currently a Professor of electrical engineering with the School of Electrical Engineering, Guangxi University, Nanning, China. His research interests include embedded power generation modeling and simulation, power quality studies, wavelet analysis, multicriteria decision-making, renewable energies, and dynamic equivalent. He is also a Fellow of the Institution of Engineering and Technology (IET), U.K., the ASEAN Academy of Engineering and Technology (AAET), and The Institution of Engineers, Malaysia (IEM), a Chartered Engineer under the Engineering Council United Kingdom (ECUK), and a Professional Engineer under the Board of Engineers, Malaysia (BEM).

SHARUL KAMAL ABDUL RAHIM (Senior Member, IEEE) received the degree in electrical engineering from The University of Tennessee Knoxville, USA, the M.Sc. degree in engineering (communication engineering) from Universiti Teknologi Malaysia (UTM), and the Ph.D. degree in wireless communication system from the University of Birmingham, U.K., in 2007. After his graduation from The University of Tennessee Knoxville, he spent three years in industry. After graduating the M.Sc. degree, he joined UTM in 2001, where he is currently a Professor with the Wireless Communication Center. He has published over 200 learned articles, including the *IEEE Antenna and Propagation Magazine*, the IEEE TRANSACTIONS ON ANTENNA AND PROPAGATION, IEEE ANTENNA AND PROPAGATION LETTERS, and obtained various patents. His research interests include antenna design, smart antenna systems, beamforming networks, and microwave devices for fifth generation mobile communication. He is also a Senior Member of IEEE Malaysia Section, a member of The Institute of Engineers, Malaysia, a Professional Engineer with BEM, and a member of the Eta Kappa Nu Chapter, The University of Tennessee Knoxville, and the International Electrical Engineering Honor Society. He is also an Executive Committee of the IEM Southern Branch.

AKRAM ALOMAINY (Senior Member, IEEE) received the M.Eng. degree in communication engineering and the Ph.D. degree in electrical and electronic engineering (specialized in antennas and radio propagation) from the Queen Mary University of London (QMUL), U.K., in July 2003 and July 2007, respectively. He joined the School of Electronic Engineering and Computer Science, QMUL, in 2007, where he is currently a Reader of antennas & applied EM. His current research interests include small and compact antennas for wireless body area networks, radio propagation characterization and modeling, antenna interactions with the human body, computational electromagnetic, advanced antenna enhancement techniques for mobile and personal wireless communications, nano-scale networks and communications, THz material characterization, and communication links and advanced algorithm for smart and intelligent antenna and cognitive radio systems. He is also an Elected Member of the U.K. International Union of Radio Science (URSI) panel to represent the U.K. interests of URSI Commission B (1 September 2014–31 August 2020).